DACITIC ASH-FLOW SHEET NEAR SUPERIOR AND GLOBE, ARIZONA

By

Donald W. Peterson

February 1961

TABLE OF CONTENTS

Table of Contents (Cont'd)

LIST OF TABLES

LIST OF ILLUSTRATIONS

List of Illustrations (Cont'd)

ABSTRACT

Remnants of a dacitic ash-flow sheet near Globe, Miami, and Superior, Arizona cover about 100 square miles; before erosion the area covered by the sheet was at least 400 square miles and perhaps as much as 1,500 square miles. Its maximum thickness is about 2,000 feet, its average thickness is about 500 feet, and its original volume was at least 40 cubic miles. It was erupted on an eroded surface with considerable relief.

The main part of the deposit was thought by early workers to be a lava flow. Even after the distinctive character of welded tuffs and related rocks was discovered, the nature and origin of this deposit remained dubious because textures did not correspond to those in other welded tuff bodies. Yet a lava flow as silicic as this dacite would be viscous instead of spreading out as an extensive sheet. The purpose of this investigation has been to study the deposit, resolve the inconsistencies, and deduce its origin and history.

Five stratigraphic zones are distinguished according to differences in the groundmass. From bottom to top the zones are basal tuff, vitrophyre, brown zone, grey zone, and white zone. The three upper zones are distinguished by colors on fresh surfaces, for each weathers to a similar shade of light reddish brown. Nonwelded basal tuff grades upward into the vitrophyre, which is a highly welded tuff. The brown and grey zones consist of highly welded tuff with a lithoidal groundmass.

Degree of welding decreases progressively upward through the gray and the white zones, and the upper white zone is nonwelded. Textures are clearly outlined in the lower part of the brown zone, but upward they become more diffuse because of increasing devitrification. In the white zone, original textures are essentially obliterated, and the groundmass consists of spherulites and microcrystalline intergrowths. The chief groundmass minerals are cristobalite and sanidine, with lesser quartz and plagioclase. Phenocrysts comprise about 40 percent of the rock, and their relative proportions are fairly uniform. Almost three-fourths of the phenocrysts are plagioclase, one-tenth quartz, one-tenth biotite, and the remainder sanidine, magnetite, and hornblende, with accessory sphene, zircon, and apatite.

Pumice fragments are nearly equidimensional near the top of the sheet, and downward they become progressively more flattened until they finally disappear. The zones and the pumice fragment flattening ratio (ratio of length to height) provide means for recognizing several faults within the sheet.

Twelve new chemical analyses are nearly uniform in composition. If named according to chemical composition, the rock would be a quartz latite, but when named according to phenocrysts, it is a dacite.

From the field occurrence and the interpretation of relict textures, it is concluded that the deposit is an ash-flow sheet containing large amounts of welded tuff, and that it was emplaced by a type of nuée ardente instead of a lava flow or air-fall shower. The nature of zoning and trend of flattening ratios indicate a series of

eruptions in rapid enough succession for the sheet to form a single cooling unit. Except in the lower part of the sheet, original textures were obscured by devitrification and crystallization during cooling. Nearly uniform mineralogy and chemistry suggest a single magmatic source. A nearly circular area, about 3½ miles in diameter, of altered dacite and earlier volcanic rocks, bounded by intricately faulted and brecciated older rocks, may be the site of a caldera that represents the source of the eruptions.

INTRODUCTION

A thick body of dacitic volcanic rock covers large areas in the vicinity of Globe, Miami, and Superior, Arizona. During the writer's assignment to geologic mapping in this area, as part of the Globe-Miami project of the U. S. Geological Survey, he became interested in the origin of this rock. This study is the result of that interest.

Within the last thirty years, sheets of silicic volcanic rock with distinctive characteristics, similar to those of the dacitic body near Superior and Globe, have been recognized in the western United States and in other parts of the world. These rock bodies differ from lava flows on the one hand and air-fall tuffs on the other, yet possess certain features common to both. In the literature of English-speaking countries they have generally been called "welded tuffs" or "ignimbrites." Explanations of their origin have required modifications of long-standing concepts of volcanism, and many recent studies have been concerned with the description and origin of these rocks. All but the most recent are listed in Cook's "Ignimbrite Bibliography" (1959). Several recent papers give excellent reviews of the development of scientific thinking on this problem; among them are those by Williams (1957), Martin (1959), Mackin (1960), Smith (1960), and Cook (1960). Each of these articles provides a good insight into the current thinking and the unsolved problems of these most interesting deposits.

Deserving of special mention, perhaps, is Smith's review article in which the mode of eruption, recognition of units, size and characteristics of deposits, source areas, origin of the magma and other problems are treated.

The chief purpose of this paper is to describe the dacitic ash-flow deposit near Superior, Globe, and Miami, Arizona. In addition, certain ideas on the origin of the deposit are advanced, and criteria for structural interpretation within the seemingly uniform part of the sheet are proposed.

Field work

The Globe-Miami project of the U. S. Geological Survey has included detailed geologic mapping of five 7½-minute quadrangles: Globe, Inspiration, Pinal Ranch, Haunted Canyon, and Superior. These quadrangles lie between 110°45' and 111°7½' west longitude and 33°15' and 33°30' north latitude, and their locations are indicated on figure 1. Nels P. Peterson has been in charge of the project since it began in 1943. Several reports on the geology of the area have been published, and others are in press. Those describing the dacite and showing its distribution include: N. P. Peterson, Gilbert, and Quick, 1951, p. 42-43; N. P. Peterson, 1954; D. W. Peterson, 1960; N. P. Peterson, in press (1) and (2). The present paper is based chiefly on the writer's mapping and studies in the Haunted Canyon and Superior quadrangles. N. P. Peterson and others have done most of the geologic mapping in the three remaining quadrangles, though the writer mapped small areas in the Inspiration and Pinal Ranch

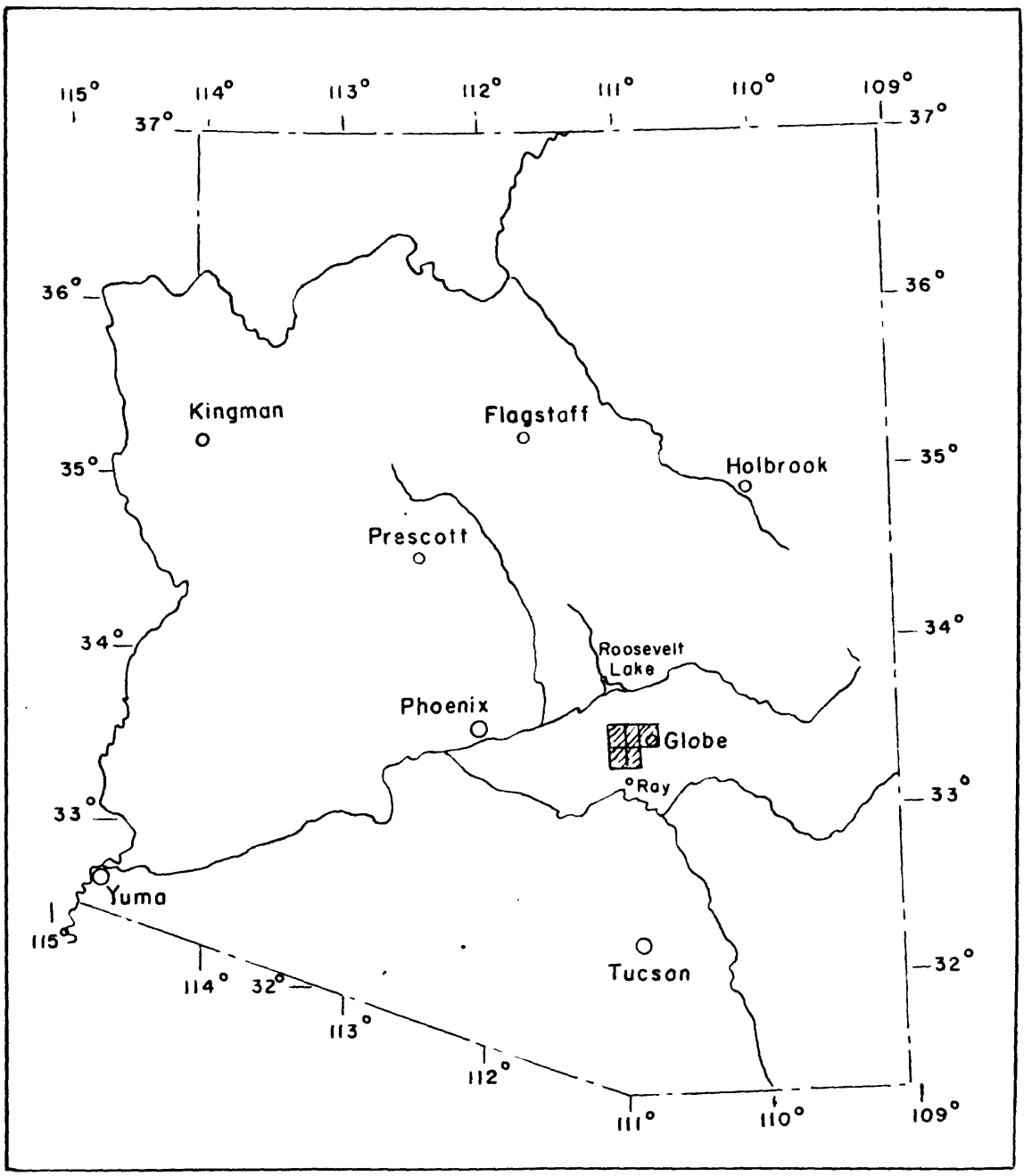

Figure 1.--Index map of Arizona, showing the location of the five 7½-minute quadrangles in which the dacitic ash-flow sheet was studied.

quadrangles and has supplemented the work by brief studies in scattered localities in each of the quadrangles. The study has been made at intervals from 1952 to 1960. Approximately eighteen months of the time spent in the field during this period has been devoted to the dacitic ash flows and closely related problems.

Previous work

The dacitic sheet was first studied in the Globe 15-minute quadrangle by Ransome (1903, p. 88-95) who identified it as a lava flow. He described three distinct phases: tuff at the base, vitrophyre, and thick dacitic flows. Several of Ransome's later papers contain descriptions of dacite, and some of his later maps show additional areas covered by the sheet, but these reports use essentially the same description as the earliest paper (Ransome, 1919, p. 68-71; 1923, p. 13).

Short and others (1943, p. 45-49) described the dacitic sheet near Superior as alternating lava flows and tuff deposits. N. P. Peterson, in his studies between 1943 and 1955, deduced that a lava as silicic as this dacite would be erupted as relatively short, thick flows, with contorted flow structures, whereas the deposit actually covers hundreds of square miles and the flow-like structures are uniformly flat-lying or gently tilted. He concluded that ash flows of a glowing-avalanche type were the most probable manner of eruption of the dacitic sheet (N. P. Peterson, in press (1)). C. S. Ross (1955, p. 431) mentioned great thicknesses of welded tuff in the Globe-Superior region of Arizona.

Acknowledgments

N. P. Peterson has maintained a continuing, encouraging interest in the study. R. L. Smith visited the area in 1957, and did much to clarify certain difficult points. Many critical discussions have been held with R. J. Roberts and H. R. Cornwall which have greatly aided the writer to develop his concepts of ash-flow deposits. R. R. Coats, J. H. Mackin, and E. F. Cook have provided additional helpful discussion and comments.

TERMINOLOGY

In new fields of investigation it seems inevitable that a certain amount of confusion of terminology develops. Different investigators, working independently, may introduce different names for the same feature, or they may use a single term in different senses. The full range of meaning, or the limitations of a newly coined term, may not be realized until after it has been used in different ways by several different workers. Each of these difficulties is well illustrated by the general subject embraced by the terms welded tuff, ignimbrite, ash flow, and other related names. The difficulties can be minimized if the terms to be used are clearly defined and used accordingly by each author.

R. L. Smith (1960, p. 800-801) has clearly defined a set of terms that he has found applicable in working with and describing these deposits, and in an effort toward attaining a uniform nomenclature, the writer intends to follow Smith's terminology as nearly as possible. Brief definitions of the terms that are most appropriate to the dacitic sheet near Superior and Globe are repeated here, and their application to the deposit is discussed.

Ash flow: The basic unit of ash-flow deposits; the deposit resulting from the passage of one nuée ardente.

Ash-flow sheet: Any unspecified sheetlike unit or group of units considered to be of ash-flow origin.

Welded tuff: A rock or rock body in which vitric particles have some degree of cohesion by reason of having been hot and viscous at the time of their emplacement.

Cooling unit: A single or multiple ash-flow deposit that can be shown to have undergone continuous cooling.

Simple cooling unit: An ash flow or sequence of ash flows that has had an essentially uninterrupted cooling history.

Compound cooling unit: One that shows departures in expectable zonation and other properties which result from simple cooling, because the intervals between ash flows were too great for readjustment to a single-unit cooling gradient.

Composite sheet: A cooling-unit complex that grades from one cooling unit into two or more cooling units.

Ash-flow field: Deposits of pyroclastic rocks consisting preponderantly of ash flows, which are related to some specific unit of area.

Before Smith's definition of "ash flow" can be fully grasped, it is essential to know precisely what he means by a "nuée ardente." Briefly, he emphasized the original observations that a nuée ardente has two parts, a basal avalanche that contains the bulk of the erupted material, and an overriding cloud of expanding gas and dust (Smith, 1960, p. 802-804). Although a nuée ardente is both a type of eruption and an agent of transport, Smith emphasizes its role as an agent of transport of material from the vent to its final resting place.

The dacitic body near Superior, Miami, and Globe forms an

"ash-flow sheet," made up of an undetermined number of separate "ash flows" that in most places cannot be individually recognized. Part of the deposit is composed of "welded tuff," and part is nonwelded. It will be shown that in most places the ash-flow sheet comprises a "simple cooling unit." It locally grades into a "compound cooling unit," but the departure from simple cooling is not great. It could be called a "composite sheet" because it shows both simple and compound cooling, but since the departure from simple cooling is small, a more accurate idea of the deposit's total character is rendered by thinking of it as a simple cooling unit. The ash-flow sheet considered in this study constitutes part of an "ash-flow field" that extends from the Superstition Mountains southeast to Ray and northeast to the Salt River 15 miles east of Roosevelt Lake.

In most of the literature describing the area, "dacite" has been used as the name for the dacitic body of rock near Superior, Globe, and Miami (Ransome, 1903, 1919, 1923; Short and others, 1943; Peterson and others, 1951; Peterson, 1954), and the name is firmly established in current local usage. Dacite may be defined as a volcanic rock with appreciable quartz phenocrysts and with its feldspar phenocrysts mostly plagioclase; dacite therefore properly describes the mineralogic composition of the rocks in this deposit. As the single word "dacite" strictly describes only the composition of the rock, and as some geologists object to applying <u>rock</u> names to <u>rock units</u>, the body of dacitic rock will be called the "dacitic ash-flow sheet," or shortened to dacitic sheet. In a different sense the rock body may be called a "cooling unit."

The term "ignimbrite"

"Ignimbrite" was proposed by Marshall (1932, 1935) as a name for the pyroclastic rocks of the rhyolite plateau on the north island of New Zealand. He defined "ignimbrite" rather broadly: Ignimbrites are rocks " . . . deposited from immense clouds of intensely heated minute fragments of volcanic magma. Temperature was so high that fragments were viscous and adhered together after falling." (Marshall, 1935, p. 323); ignimbrites are "igneous rocks of acid or intermediate composition which have been formed from material that has been ejected from orifices in the form of a multitude of highly incandescent particles which were mainly of a minute size." (1935, p. 357); "Ignimbrite is used as a name for a tufaceous rock of acid composition that has been formed from a 'nuee ardente Katmaienne' . . . " (1935, p. 360).

From Marshall's classification of ignimbrites, it is clear that he intended the term to apply to both welded and nonwelded tuffs (Marshall, 1935, p. 357-360). Several authors have unfortunately used "ignimbrite" as a synonym for "welded tuff," though this usage is contrary to Marshall's intent. Stressed in each of Marshall's definitions is that ignimbrite is a rock formed by a nuée ardente of the Katmai type. Ignimbrite, therefore, is strictly a genetic term.

Cook has proposed that ignimbrite be redefined to apply to pyroclastic rock units of probable nuée ardente origin (Cook, 1955). Ignimbrite in this sense is a term for a stratigraphic unit, and the rocks that comprise the unit are individually designated according to their composition, size of particles, and degree of welding. They

might include either welded or nonwelded tuff, or both. Cook (1957, 1960), Martin (1959), Mackin (1960), and others have used ignimbrite in this way, and in general it seems to be a satisfactory way in which to designate stratigraphic units. In complex volcanic fields, however, the above definition does not specify just what constitutes a single ignimbrite, or how seperate ignimbrites are to be established or identified. Although the rock deposit of the present study can be designated as "an ignimbrite" according to Cook's definition, because of potential complications in the volcanic relations of nearby areas, the writer has selected to follow the nomenclature system proposed by Smith (1960, p. 800-801).

FIELD DESCRIPTION OF THE ASH-FLOW SHEET

Distribution, area, thickness, and volume of the deposit

Dacitic ash-flow deposits originally covered an area of at least 400 square miles in the Globe-Superior area, but erosion has reduced the present outcrop area to about 100 square miles (plate 1). It is possible that the deposits originally covered a much greater area, perhaps 1,500 square miles, but correlations have not been established with rocks of similar appearance that lie to the northwest in the Superstition Mountains and to the west, southwest, and northeast.

The largest continuous area now covered by the ash flows lies northeast of a line between Superior and Ray, and extends eastward to the Dry Wash Fork of Mineral Creek, and northward to Powers Gulch and Wood Creek. Other large remnants of the mass lie between Haunted Canyon and the West Fork of Pinto Creek, along Pinto Creek near Cold Gulch, and in the area around Webster Mountain, upper Eastwater Canyon, and Day Peaks. Smaller patches lie north of Globe and Miami, and others are scattered through the area shown in plate 1. Part of a large ash-flow remnant crosses the northwest corner of the map of plate 1.

Thickness of the ash-flow sheet depends both on irregularities of the surface at the time of eruption and on subsequent erosion. Because of the underlying relief, original thickness was variable;

furthermore, the eroded upper surface prohibits accurate determination of the complete range of original thickness. In a few places, however, rocks lying close to the original upper part of the unit are preserved, and original thickness can be estimated. The ash-flow sheet is thickest just east of Superior where it reaches about 2,000 feet. In each of the larger areas of outcrop, thicknesses of over 1,000 feet are common, and the average thickness of the sheet is estimated to have been about 500 feet.

The trends of variation in thickness of the ash-flow sheet can be only roughly indicated because of post-volcanic deformation and erosion, and scanty subsurface information. The large body of dacite east of Superior appears to be quite thick over most of its extent, and drill holes in Devil's Canyon and near the J I Ranch show it exceeds 1,500 feet. It becomes thinner toward the southeast, and is about 800 feet thick near the south border of the Superior quadrangle. On Sawtooth Ridge the dacite is about 1,300 feet thick. Eastward from Sawtooth Ridge the thickness fluctuates, but becomes progressively thinner; on JK Mountain it is 400 feet, on Webster Mountain about 500 feet, and on Sleeping Beauty about 300 feet. It is likely that the outcrop east of Globe is not much thinner than it was originally, and it is now about 160 feet thick; this suggests that this outcrop is relatively near the eastward margin of the ash flow. Data on the thickness variations outside the mapped area are not available.

If the deposit originally covered 400 square miles, and had an average thickness of 500 feet, its volume would have been 40 cubic miles, or 165 cubic kilometers.

Age

The age of the dacitic ash-flow sheet is uncertain. Ransome (1903, p. 94-95) assigned a provisional age of Tertiary to the unit because it is definitely older than the present topography and because it covers eroded Mesozoic intrusive rocks. More recent studies, including the present, have yielded no evidence to indicate the age more precisely. An absolute age determination by radioactive isotope methods is planned.

Zoning of the ash-flow sheet

Introduction

In most areas the dacitic rock forms blocky to rounded outcrops intersected by a distinct joint pattern. In areas of gentle relief, the ground surface is strewn with boulders that measure up to tens of feet across. On steeper slopes the rock forms ledges, and in rugged topography it forms ridges, peaks, and cliffs (figure 2).

Five separate zones can be recognized within the ash-flow deposit; distinction between them is based on differences in the character of the groundmass. The zones are, from bottom to top: (1) basal tuff,--poorly to moderately consolidated, non-welded dacite tuff; grades upward to (2) vitrophyre,--streaky to uniform highly welded dacite tuff, with groundmass of black glass; abrupt transition to (3) brown zone,--firmly welded dacite tuff with light brown aphanitic groundmass; grades upward to (4) gray zone,--firmly to moderately welded dacite tuff with pale red to light brownish gray aphanitic groundmass; grades upward to (5) white zone,--moderately welded to nonwelded dacite

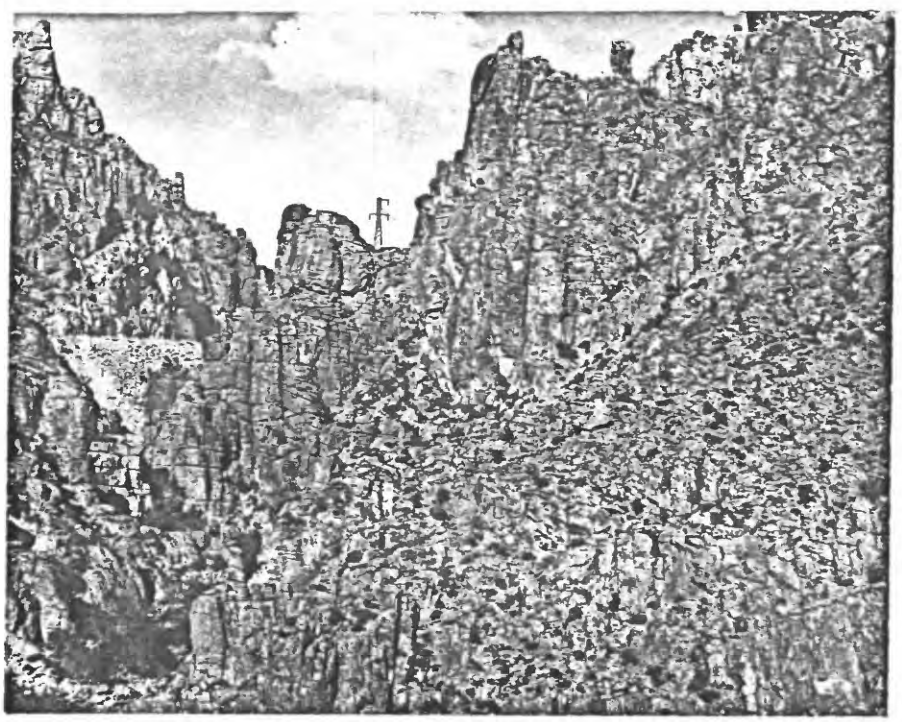

Figure 2.—Queen Creek Canyon, east of Superior. These rocks are mostly in the gray zone, but the lowermost rocks in the photograph are grading into the brown zone.

tuff with light gray to white aphanitic groundmass.

The five zones have certain features in common. Each is porphyritic with a similar phenocryst assemblage; in hand specimen phenocrysts can be identified as feldspar, quartz, biotite, accessory magnetite, and lesser amounts of hornblende and sphene. The phenocrysts comprise from one-fourth to nearly one-half the volume of the rock. They range in size from barely discernible with the hand lens up to about 3 mm, and most are one-half to 1 mm in diameter.

Lithic inclusions are common in all the zones, and locally they are abundant. Although most are angular chips a fraction of an inch in diameter, they range in size up to several inches across, and scattered boulders up to several feet in diameter have been observed. On the average, inclusions comprise 2 to 4 percent of the volume of the rock, but locally they reach 15 to 20 percent. The most abundant inclusions are rhyolite, probably derived from the earlier volcanic rocks; other common inclusions are diabase, quartzite, limestone, schist, and granular igneous rocks, all of which crop out in the surrounding area.

Basal tuff

At every locality where the base of the ash-flow sheet is exposed, it consists of nonwelded crystal tuff; none of the overlying units has been observed in depositional contact with older rocks. This tuff is poorly to moderately indurated, and weathers to gentle, subdued slopes. It commonly is covered by talus from the overlying, more resistant rocks. It is generally non-bedded, though in some places it

consists of bedded lenses or layers of tuff that may be mixed with clastic sediments. Both weathered and fresh surfaces are light gray to white, and they may grade to shades of yellowish gray and moderate red. The basal tuff ranges from 2 to over 100 feet in thickness, and averages between 10 and 20 feet. Figure 3 shows a three-foot layer of tuff.

In the most common variety of tuff, the phenocrysts lie in a light colored, powdery matrix whose texture is generally quite uniform (figure 4). The rock may contain variable amounts of pumice lapilli and blocks, ranging from a fraction of an inch up to several inches in diameter. In some places the uniform texture and structure gives way to a heterogeneous mixture of abundant lithic inclusions, assorted pumice lumps, and phenocrysts in the fine powdery matrix.

Constituents of the lower part of the basal tuff are randomly oriented, but upward the pumice tends to be flattened. The tuff becomes more firmly consolidated upward, specific gravity increases, and 1- to 10-mm streaks of black glass appear, which become more abundant upward. These changes mark the gradational transition from tuff to vitrophyre; the transition zone in some places is one or two feet thick and in other places is as much as 30 to 40 feet thick.

Vitrophyre

A layer of porphyritic glass lies between the basal tuff and the overlying lithified zones, and it apparently extends continuously over the entire area of the ash-flow sheet. The vitrophyre is generally so firm and resistant to weathering that it commonly stands out

Figure 3.—Base of the ash-flow sheet in Devils Canyon near the south edge of the Superior quadrangle. Whitetail conglomerate is overlain by a 3-foot light-colored layer of basal tuff which grades upward through about 8 feet into vitrophyre. The vitrophyre is dark-colored and shows well-developed polygonal columnar structure. A nodular layer separates the vitrophyre from the overlying brown zone. Hammer near left edge on basal tuff shows scale.

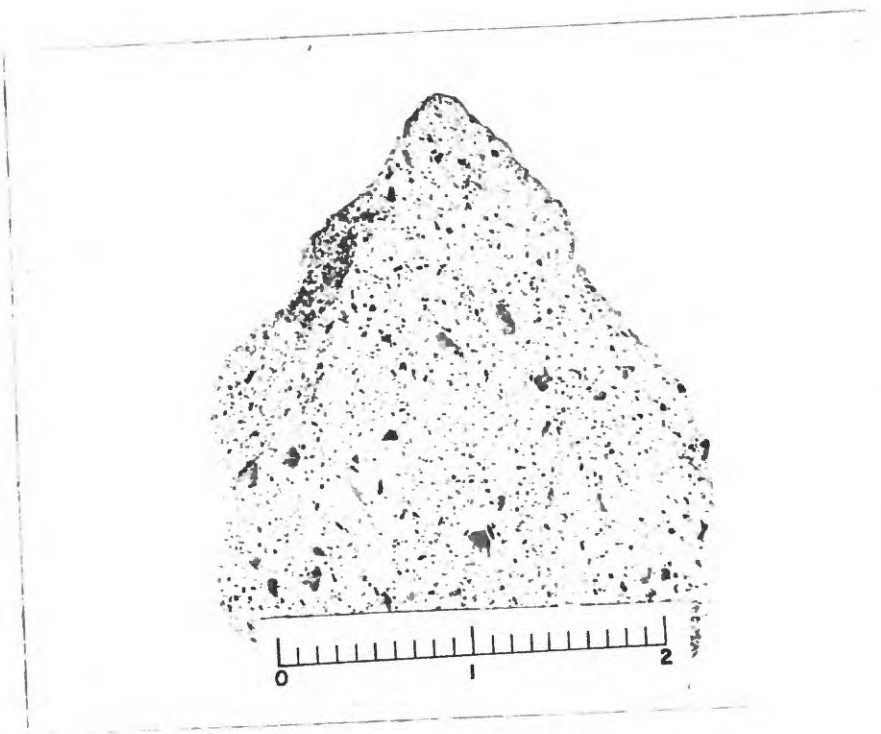

Figure 4.—Hand specimen of basal tuff. Scale in inches. Photograph by Elliot C. Morris.

as a ledge or as distinct outcrops above the basal tuff (figures 3 and 5). In some places, however, it crumbles easily and may be covered by debris from above. It weathers to a dark gray or dark brown color, and it contrasts distinctly with the lighter colored rocks above and below. The fresh surface typically is shining black mottled with light colored phenocrysts (figure 6), but it varies to black streaked with abundant brown lenses. The vitrophyre ranges from 2 to 80 feet in thickness, and averages between 5 and 25 feet.

The vitrophyre typically consists of phenocrysts set in a matrix of uniform, black glass. Megascopically the glass appears to be massive and uniform, but the microscope reveals the layered and deformed fragmental textures that are characteristic of very firmly welded tuffs. In some places the glass shows perlitic structure. Gradational between the massive vitrophyre and the underlying tuff are streaky phases of vitrophyre, consisting of alternating, irregular layers and lenses of black glass and brown to gray aphanitic material. In many places, especially where it is thin, the vitrophyre consists entirely of this streaky phase.

The vitrophyre and the brown zone generally contain more lithic inclusions than the other zones. Precise counts have not been made, but it is estimated that most of the vitrophyre contains 5 to 10 percent of xenoliths.

Small spherical nodules are common in some localities in the vitrophyre; they contain the same assemblage of phenocrysts set in a brown, aphanitic groundmass. The nodule boundaries are sharp and

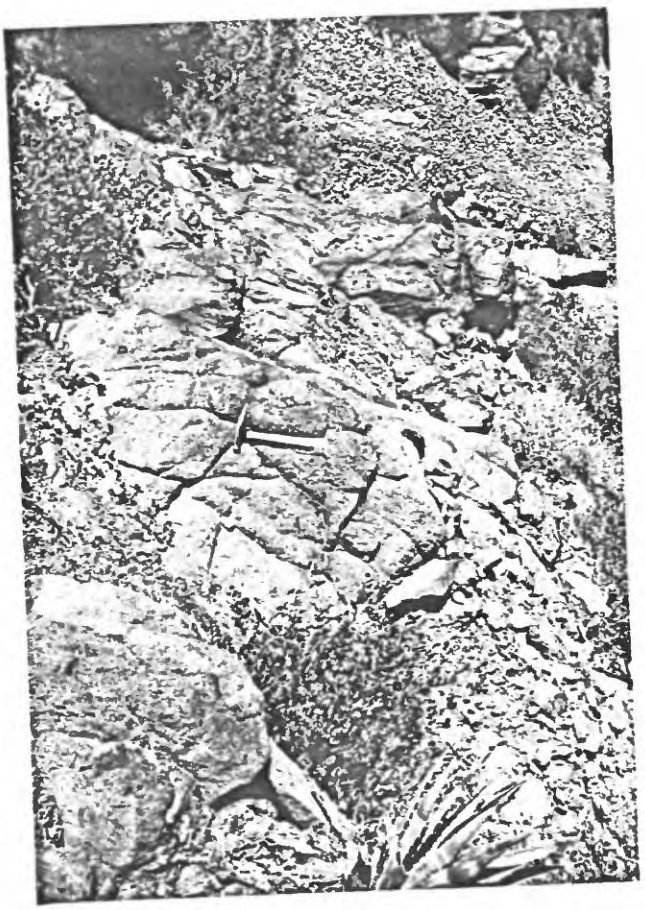

Figure 5.—Vitrophyre outcrop near Queen Creek.

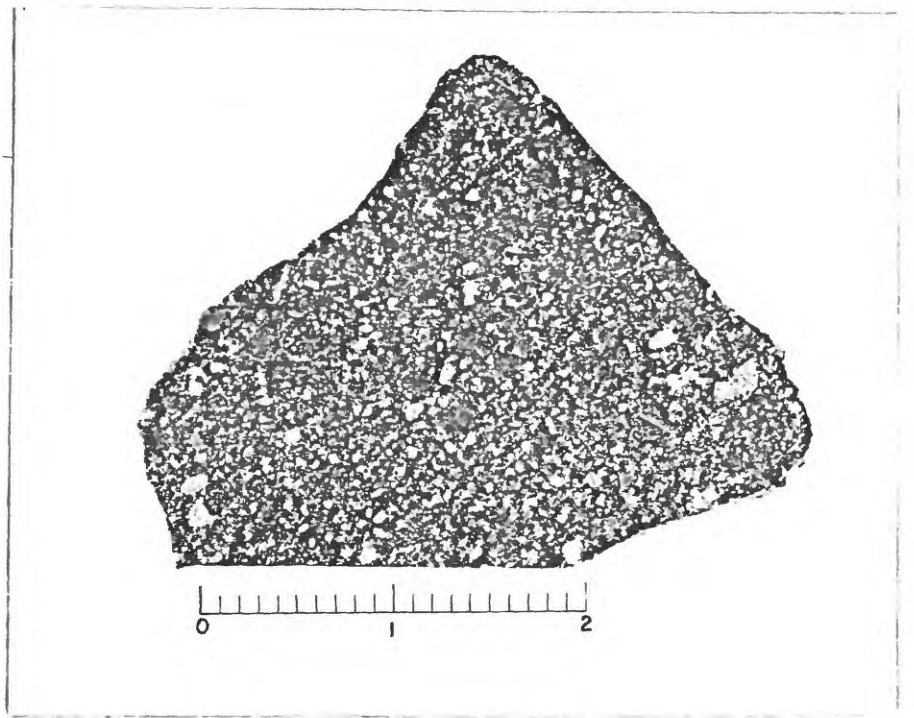

Figure 6.—Vitrophyre hand specimen. Scale in inches. Photograph by Elliot C. Morris.

distinct; they generally are more resistant than the surrounding glass and stand out as bumps on the weathered surface. Their centers are generally occupied by a dusty powder, which is immediately removed by weathering when exposed at the surface, so weathered cross sections of the nodules appear to be hollow. The nodules commonly range from a fraction of an inch to about 4 inches in diameter, but some reach several feet in diameter. In most places they comprise only a fraction of a percent of the volume of the rock, but locally they increase in abundance to several percent.

In a few places the vitrophyre is cut by well developed columnar joints. These joints define individual polygonal columns, a foot or less in diameter and 10 to 40 feet or more in height (figures 3 and 7). A single joint surface lies between two columns only, and each joint is intersected by other similar joints at the corners of the polygons. This type of jointing is typical of basaltic and andesitic lavas, and has also been observed in many ash flows; it is generally considered to have developed due to contraction of the rock during cooling. With one exception, columnar jointing in this area has been observed only in the vitrophyre unit. It does not extend up into the brown phase, and generally dies out downward into the underlying partly welded tuff.

Over most of the area, basal tuff grades upward into a single vitrophyre layer, which in turn is overlain by the brown zone of dacite. In some areas, however, above the basal tuff a lower vitrophyre layer grades upward into an intervening layer of tuff, which in turn grades upward into a second vitrophyre layer. The intervening tuff pinches

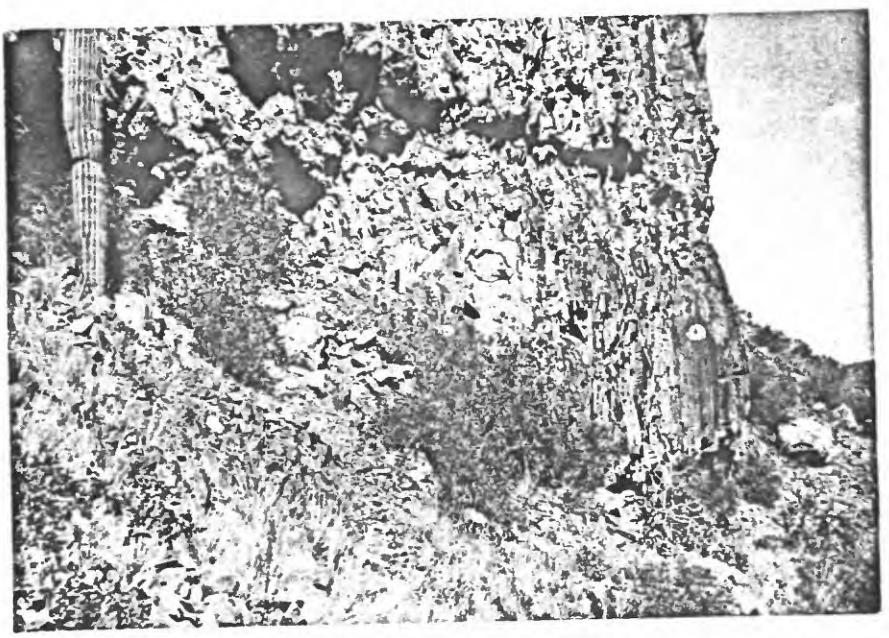

Figure 7.—Polygonal columnar structure in the vitrophyre overlain by the nodular layer at the base of the brown zone, near the south edge of the Superior quadrangle.

and swells irregularly, and reaches a maximum thickness of about 15 feet. The lower vitrophyre is generally only a few feet in thickness, but the upper vitrophyre ranges from a few feet to several tens of feet in thickness. Exposures studied have been inadequate to establish definitely the lateral extent of any particular layer of intervening tuff, but some may extend for several hundred feet, and others may extend even farther. In the area from King's Crown Peak southward to beyond Queen Creek, nearly every complete exposure of the vitrophyre contains a layer of tuff between upper and lower vitrophyre. An intervening tuff has also been noted along the west boundary of the dacite between Haunted Canyon and the West Fork of Pinto Creek, particularly near Rock Creek and on Sawtooth Ridge. At the east end of this body, on the south flank of Government Hill, three distinct layers of vitrophyre are separated by partly welded tuff.

The contact between the vitrophyre and the brown zone of dacite is generally not exposed. The contact is apparently abrupt, for typical vitrophyre commonly lies within two or three feet of lithic dacite, but the actual contact in most places is persistently hidden. In a few places, incomplete exposures reveal a crumbly, partly glassy and partly lithoidal rock at this contact. Near the south end of Devil's Canyon, however, this contact is well exposed, and it consists of a remarkable layer of nodules 1 to 5 feet in diameter (figures 3, 7, and 8). The layer is from 2 to 8 feet in thickness; it persists over a lateral distance of more than a mile without interruption, and continues southward an undetermined distance. The nodules are composed of rock

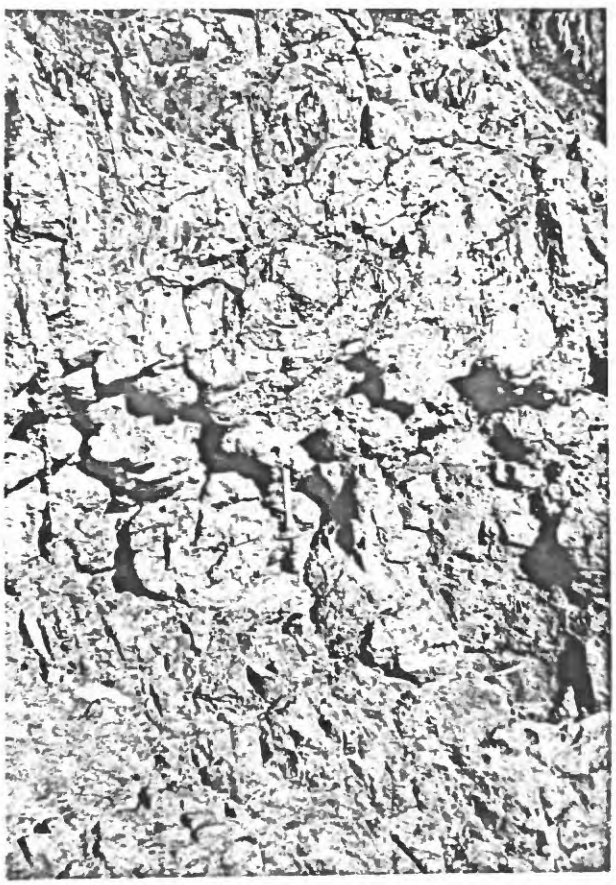

Figure 8.--Nodular layer at base of brown zone above vitrophyre near south edge of Superior quadrangle.

identical to the brown zone of the dacite, and the material between them is altered, crumbly, devitrified glass. The nodules were probably formed during devitrification caused by gases.

Brown zone

In most areas, the lithified dacite immediately above the vitrophyre is light brown, reddish brown, or yellowish brown, and it is designated as the brown zone (figure 9). It generally is hard, flinty, and resistant to weathering, and stands as steep slopes and ledges, though locally it is soft and non-resistant. It weathers to shades of brown and grayish brown, and weathered surfaces are commonly not distinguishable from the overlying units. Because of the indefinite upper boundary, it is not possible to state the thickness precisely but the general range is 20 to 200 feet. In some places the brown zone may reach 300 feet in thickness; in other places it pinches out or is poorly defined where the ash-flow sheet is thin.

The rock of the brown zone consists of phenocrysts set in a dense, aphanitic, brownish orange matrix (figure 10). In some places its texture appears almost massive and uniform, but in most places the hand lens reveals a discontinuously layered or foliated texture, formed by flattening of volcanic particles. Although the microscope shows that much of the matrix is glassy, it is partly devitrified, and the aspect of the rock is distinctly stony or lithoidal.

Like the vitrophyre, the brown zone commonly contains more lithic fragments than the other zones. Lithic fragments commonly comprise about one-tenth of the rock, and locally they reach as much

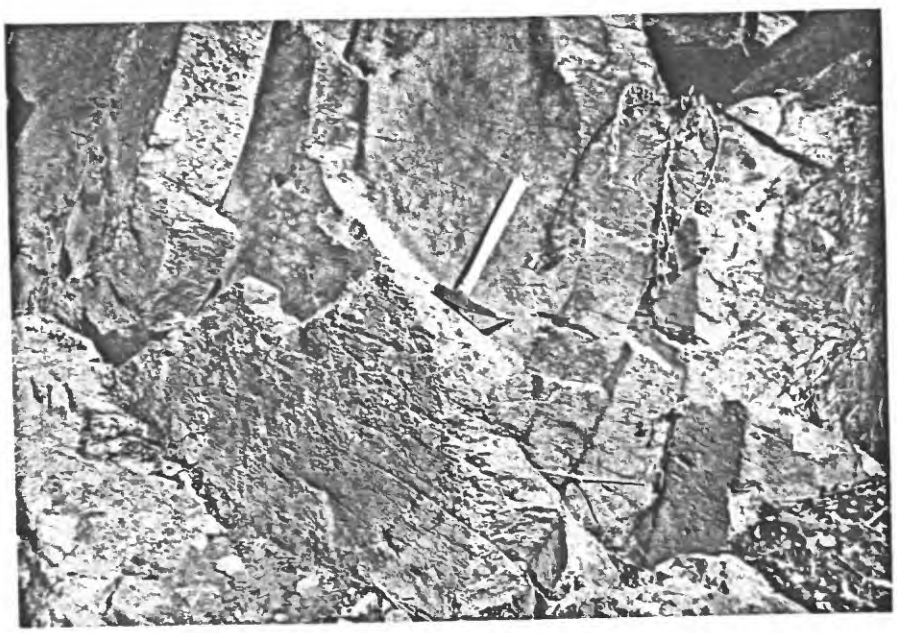

Figure 9.--Highly welded tuff in the lower part of the brown zone. Approximately 3 miles northeast of King's Crown Peak, Superior quadrangle.

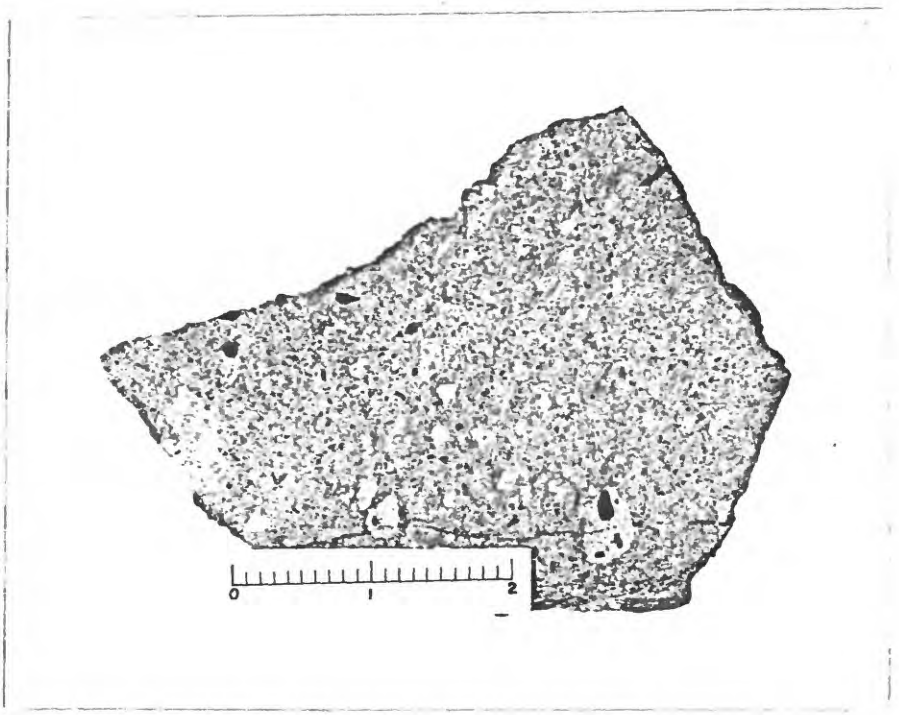

Figure 10.—Hand specimen from brown zone. Scale in inches. Photograph by Elliot C. Morris.

as a fourth. The abundant lithic fragments seem to occur in poorly-defined pockets that are irregular in size, shape, and thickness. Upward in the zone their abundance decreases. A possible explanation for the concentration of lithic fragments in the vitrophyre and brown zones is that the vents were "clearing their throats" during the earlier phases of the eruption.

No definite upper limit to the brown zone can be established, for the change from brown to the overlying gray is completely gradational. Megascopically, the transition consists of an increasing duskiness in the color of the brown lenticles, and the gradual appearance of light colored streaks parallel to the foliated structure. Distinctly brownish lenticles progressively diminish upward, but persist far up into the gray zone. Where individual zones were mapped east of Superior, placement of the contact between the brown and gray zones was largely subjective because of the gradational transition.

Gray zone

The lithoidal dacite that generally comprises the thickest zone of the ash-flow sheet is a pinkish gray, firmly welded tuff. It is a hard, resistant rock, weathered surfaces are rough, and it commonly stands as steep, rugged slopes topped by ridges and peaks (figure 2). The pattern of outcrop is commonly controlled by a pervasive system of nearly vertical joints that is apparently tectonic rather than due to cooling. The joint system is crossed by a crudely developed, but distinct, layer-like structure, generally nearly horizontal. This structure is apparently a parting parallel to the

flattened constituents. The rock weathers to shades of brownish gray and pinkish gray, and weathered rocks merge imperceptibly in color with those of the overlying and underlying zones. The fresh surface is pinkish gray, and in some places is streaked with light-gray to white flattened pumice fragments (figure 11). Generally the gray zone is the thickest zone of the sheet, locally reaching thicknesses of over 1,000 feet. A minimum thickness is difficult to specify because of the eroded upper surface. However, east of Globe the gray zone loses its distinct identity; a streaky brownish grayish zone just above the vitrophyre is only a few feet thick, and it abruptly grades upward into the white zone. It appears that the brown and gray zones tend to merge and finally pinch out where the sheet is thin.

The gray zone consists of phenocrysts set in a pinkish gray, aphanitic matrix. The texture is commonly indistinctly layered or foliated, and megascopically it appears as a rather wavy, subparallel planar texture of brownish to pinkish layers in a gray matrix. In some specimens it strongly resembles true flow structure, but careful scrutiny generally reveals that the layers are discontinuous. Upward, the brownish and pinkish layers assume a dusky gray color, but the indistinct planar textures remain perceptible. The rock is lithoidal in aspect, and the microscope shows that the groundmass is cryptocrystalline.

Flattened pumice fragments are common in the gray zone. Those lowermost in the section are extremely flattened white disks, several centimeters in diameter and less than a millimeter thick. Upward they

Figure 11.—Hand specimen from gray zone. Scale in inches. Note the flattened pumice fragments. Photograph by Elliot C. Morris.

become progressively less flattened, gradually changing to lenticular ellipsoids up to a few centimeters in diameter and 2 or 3 centimeters thick. Xenoliths are common but now abundant in the grey zone; they comprise perhaps 1 to 3 percent of the rock.

Most phenocrysts in the gray zone appear fresh, but progressing upward from the brown zone to the gray zone, biotite gradually loses its shining black or dark brown color and takes on a golden or light brown glint. Most of the biotite in the gray zone is slightly to moderately altered.

The gray zone grades upward into the white zone, and like its lower boundary, its upper boundary generally cannot be precisely located. The gradation consists of the appearance of very light gray material between the medium gray layers; these increase upward, and the proportion of medium gray material decreases. Farther upward the entire rock is very light gray, nearly white. In a few places a major change is rather abrupt, taking place across about ten feet, and although successive changes continue above and below this horizon, it is a convenient place to locate the boundary. At most places, however, the change is gradational over several hundred feet.

White zone

At the top of the ash-flow sheet is the white zone. The fresh rock is soft and non-resistant, but when exposed to weathering a hard layer coats the surface, with the result that most outcrops stand just as prominently as do those of the underlying, inherently harder rocks (figures 12 and 13). The white zone is cut by the same system of

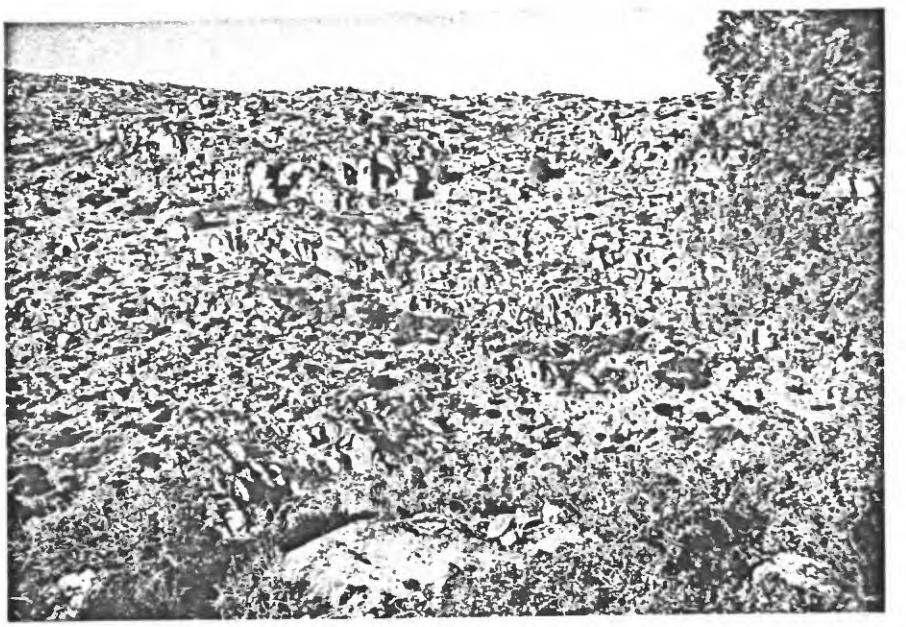

Figure 12.—Typical white zone outcrops north of Oak Flat, Superior quadrangle.

Figure 13.—Moderately welded but highly indurated rock of the white zone, on ridge east of Pinto Creek, about 2 miles south of Horrell's Ranch, Inspiration quadrangle.

vertical tectonic joints that cuts the gray zone, and these generally control the pattern of outcrop. The near-horizontal system is generally indistinct, probably because of the smaller amount of flattening of constituents. Weathered surfaces are brownish grey to pinkish gray, practically the same color as the weathered gray zone. Upward the weathered surface gradually becomes a lighter color, until near the top the color is a pale pinkish brown, distinctly lighter than the rocks lower in the section. The fresh surface is very light gray to white (figure 14). The white zone has a maximum thickness of perhaps 800 feet, and averages 200 to 300 feet. Again, the thicknesses are uncertain because of the gradational lower contact and the eroded upper surface.

The rock of the white zone consists of pherocrysts set in a very light gray to white, aphanitic matrix. In general no layered structure is perceptible, and the rock has a uniform, massive structure, but as the rock grades downward into the gray zone, a discontinuous irregular layered structure becomes distinct. The bulk of the white zone is firm and tough, yet its fresh surface is rather soft. Its induration is largely due to crystallization rather than welding. Spherulites and irregular masses of fine microcrystals are abundant, and show that the groundmass is considerably crystallized.

Pumice fragments are abundant; they are only slightly flattened in contrast to the more thoroughly flattened fragments lower in the section. On the fresh surface the pumice fragments are nearly the same color as the enclosing rock, and in some places they are difficult

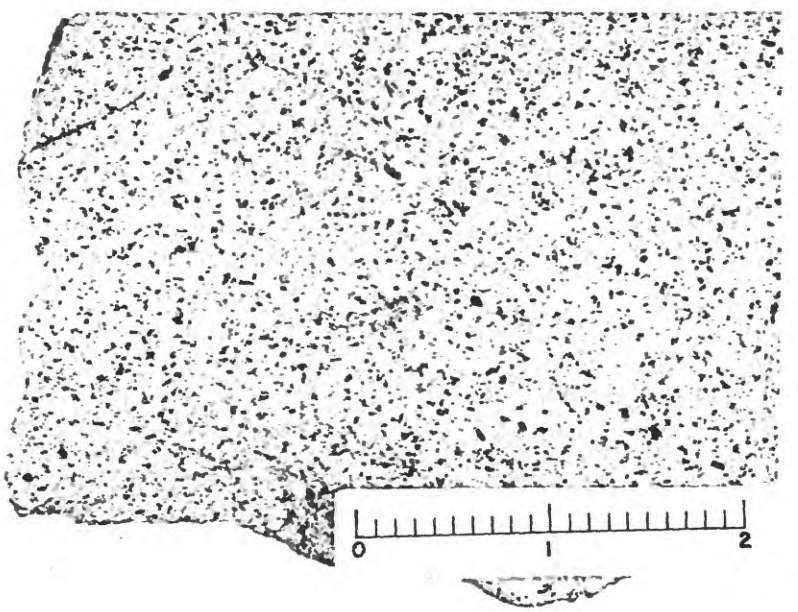

Figure 14.—Hand specimen from white zone. Scale in inches. Photograph by Elliot C. Morris.

to distinguish. However, the fragments weather to a lighter shade and generally show clearly in outcrop. Their susceptibility to weathering varies; in some places they weather away quickly and leave a surface pock-marked with cavities, and elsewhere they show about the same resistance as the rock that surrounds them. Xenoliths comprise about 1 to 3 percent of the rock. Ellipsoidal gas cavities are fairly common; some are lined or filled with small quartz crystals, and others are filled with light gray to brown powdery material.

Progressing upward from the gray to the white zone, biotite phenocrysts become more and more altered, gradually changing from golden brown flakes to dull dark brown aggregrates composed chiefly of iron oxide. The other phenocrysts remain fresh and unaffected by alteration.

In most places the white zone has been deeply dissected or largely removed by erosion. A thick section of the white zone crops out east of Superior, however, and in the vicinity of Oak Flat it is likely that rocks representing the original top of the section are preserved. The uppermost part of the white zone is composed of white, punky tuff with low specific gravity, but it resembles the lower part of the white zone in composition and texture. At Oak Flat the white zone is overlain by layers of ash with distinct bedding; a sharp contact marks the base of the ash, which has been mapped as a separate unit.

Pumice fragments

Field occurrence and distribution

Light-colored cognate inclusions are locally abundant in the lithic parts of the dacitic ash-flow sheet. Hansons described them as "small streaks or blotches of nearly white material" (Hanson, 1919, p. 69; 1923, p. 13). They were briefly described by N. P. Peterson and others (1951, p. 42) as follows: "In some very clean outcrops, what appear to be the shadowy outlines of dacite fragments are visible, suggesting that part of the rock is a firmly welded agglomerate." The fragments are lenticular and ovoidal in shape; toward the top they are nearly equidimensional and downward they are progressively flattened. Most of them range from one to four inches in their longest dimension, but both larger and smaller sizes are common. In general their light color contrasts with the slightly darker colored dacitic matrix. Most of them carry approximately the same assemblage of phenocrysts in about the same proportions as the matrix, and except for their lighter color appear to be practically the same rock.

Lenticular inclusions of this type are apparently very common in ash-flow sheets. A few of the papers that mention and describe lenticular fragments are those of: Marshall, 1935, p. 332-335; Gilbert, 1938, p. 1635; Enlows, 1955, p. 1224-1231; Cook, 1957, p. 53-58, fig. 17; and Mackin, 1960, p. 89-95. Martin has suggested that most lenticles are of two principal types: "(1) collapsed pumice lenticles, formed of flattened and welded glass and pumice lapilli; and (2) lithophysal lenticles, formed by crystallization in local pockets." (Martin,

1959, p. 405). Martin emphasized that the two types are commonly similar in appearance and difficult to distinguish from each other, and he discussed criteria for their recognition (p. 405-407).

Although their original textures have been obliterated by crystallization, the great majority of the lenticles in the ash-flow sheet of the Globe-Superior region are considered by the writer to be collapsed pumice lenticles. The principal evidence supporting this view is that most lenticles contain phenocrysts, and phenocrysts would have no chance to develop in lithophysal cavities. Although some lenticles do not contain phenocrysts and perhaps represent lithophysal crystallization, most of the lenticles are regarded as cognate pumiceous fragments.

The lenticles are not uniformly distributed through the sheet. They are most common in the white and gray zones, rare in the brown zone, and essentially absent in the vitrophyre and basal tuff. Moreover, their abundance varies within the white and gray zones; in some localities they comprise nearly one-fourth of the rock, and in other places they are scarce. In general the lenticles are especially abundant in the area of Superior and Devils Canyon, and in the areas of Pinto Creek, Webster Mountain, and vicinities. Eastward they become more scarce, and near Globe the lenticles are practically absent.

In cliff faces along Apache Leap, Queen Creek Canyon, and Devils Canyon, some successive layers of dacite may erroneously appear to contain widely different amounts of pumice fragments. When viewed from a distance, certain layers have highly pitted weathered surfaces,

the pits representing weathered-out pumice lenticles. Adjacent layers above and below show few or no pits. At spots accessible for closer examination, however, the adjacent layers were found to contain just as many lenticles as the pitted layers; apparently the difference in appearance is caused by the character of the weathering. The underlying cause of this weathering difference is not known. Sporadic attempts at mapping these layers to determine their distribution have not been successful; the locally distinctive layers commonly lose their identity when traced laterally. Many are inaccessible, and they cannot be distinguished on subdued slopes.

Flattening of the pumice fragments

In the upper part of the white zone, pumice fragments tend to be nearly equidimensional in shape and show little preferred orientation (figure 15). Lower in the white zone the fragments become slightly flattened, with ovoidal shapes, and are oriented with their longer dimension in the horizontal plane (figure 16). Further downward the flattening increases, until well down in the gray zone and into the upper part of the brown zone the flattening has become extreme, and the fragments are streaks and stretched-out lenses (figure 17). Lower still they may be represented by a mere coating on horizontal parting surfaces, and finally they completely disappear.

Cross sections of fragments exposed on surfaces parallel to the flattening are practically equidimensional, indicating that the flattening is a foliation, not a lineation (figure 18). The lack of lineation suggests that the material was deformed only in response

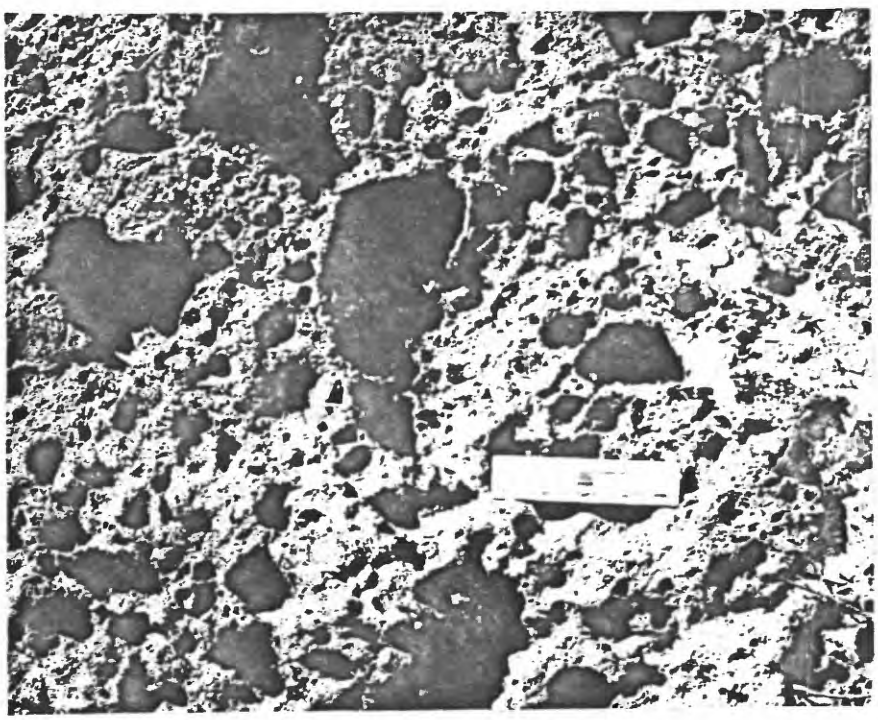

Figure 15.—Nearly equidimensional, weathered-out pumice fragments near the top of the ash-flow sheet, at Oak Flat, Superior quadrangle. Scale is 6 inches long.

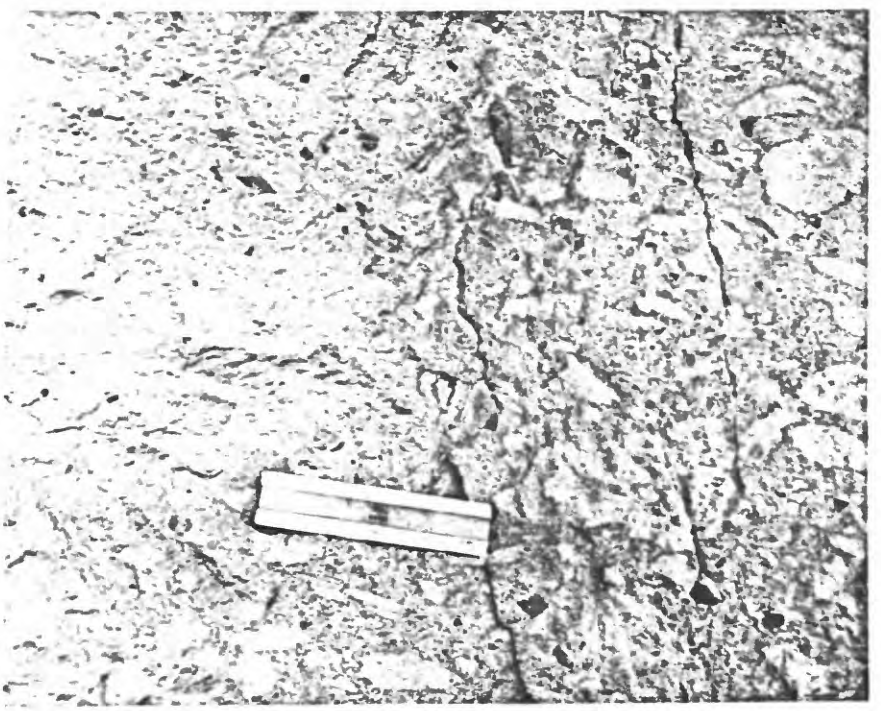

Figure 16.—Partly flattened pumice fragments, several hundred feet below the top of the ash-flow sheet. One-half mile west of Oak Flat, along U. S. highway 60-70, Superior quadrangle.

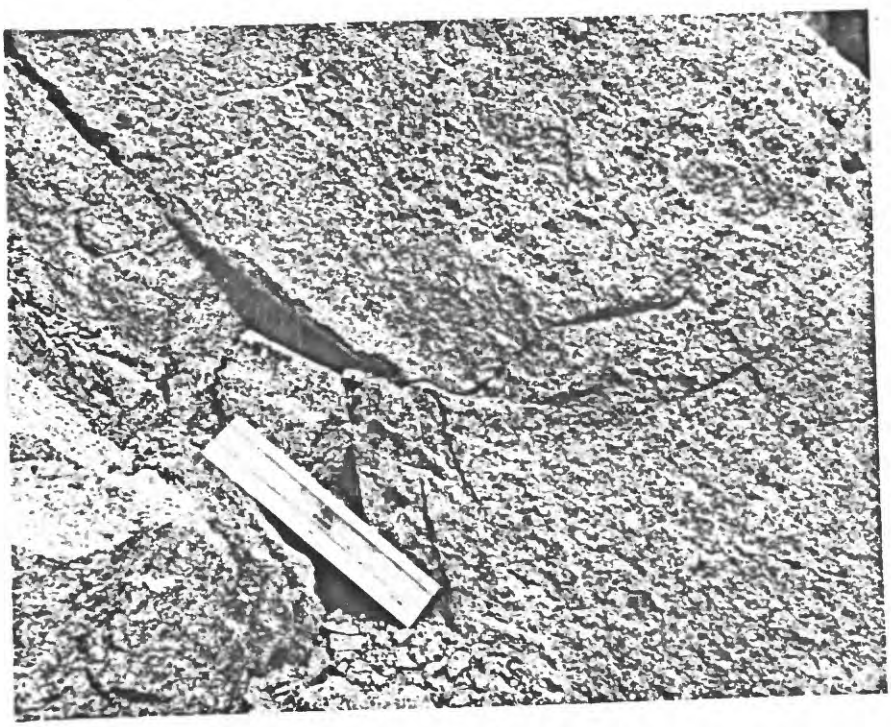

Figure 17.—Extremely to moderately flattened pumice fragments, about 1,300 feet below the top of the ash-flow sheet, at locality SHa7, near the east end of Queen Creek tunnel, U. S. highway 60-70, Superior quadrangle.

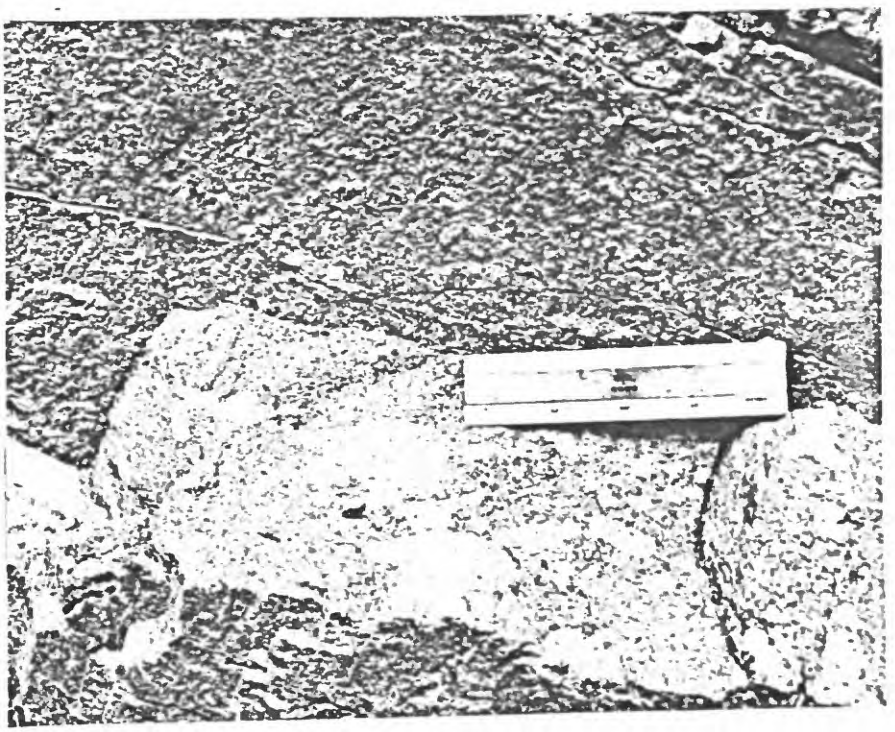

Figure 18.—The nearly horizontal surface below the scale, parallel to the flattening, shows equidimensional cross sections of pumice fragments, indicating no appreciable lateral flow. The vertical surface above the scale, similar to that of figure 17, shows highly flattened cross sections.

to the vertically superimposed load.

Although the downward trend seems to consist of a progressive increase in flattening, in any single outcrop individual fragments vary widely in the amount of flattening, and simple field observation is not sufficient to determine if the downward increase in flattening is systematic. Several localities where a considerable thickness of the ash-flow sheet is exposed were selected to test the apparent increase of flattening. Fragments were measured at successive horizons up through each section. A compilation and comparison of the measurements confirm that the flattening increases as the distance from the top of the sheet increases, and shows furthermore that the amount of flattening is an approximate guide to the distance below the top.

Measurement of the fragments

The length of a fragment may be divided by its height to give a quotient, which in this paper is called the "flattening ratio." An undeformed equidimensional fragment would have a flattening ratio of one, and if slightly deformed its flattening ratio would be slightly greater than one. Highly deformed fragments have flattening ratios up to 50 or more. Although the original shapes of the fragments introduce unknown errors into the use of these ratios, the errors are probably small. In the Oak Flat area, for example, fragments near the top of the sheet have ratios close to one (figure 15).

At each spot selected for study, the height and length of 30 or 40 fragments as exposed in a vertical face of an outcrop was measured. The flattening ratio of each fragment was calculated, and

the average flattening ratio for each particular spot was determined from the sum of the individual flattening ratios. Plate 2 shows the relation between the average flattening ratio and the stratigraphic level for six separate cross sections in various parts of the ash-flow sheet. The vertical scale is the stratigraphic distance above the base, and the horizontal scale shows the flattening ratio plotted on a logarithmic base. The locations of these studies are shown in figure 19.

The curves show that the mean flattening ratio progressively increases downward in the section. Curves SH, EC, and JK form nearly straight lines, and curve DC deviates only slightly. Curves SH, EC, JK, DC, and SS all slope consistently in the same direction, and have approximately the same amount of slope. Curve EDa shows a reversal of slope adjacent to local steepening, but the upper and lower parts resemble the other curves.

The flattening ratio of each measured fragment is also shown on plate 2 to illustrate the distribution of values at each locality. The standard deviation has been calculated, and 95 percent confidence limits based on the distribution of each assemblage are indicated on the diagrams.

In selecting outcrops on which to measure fragments, care must be taken that the exposed surface is normal to the plane of the flattening; otherwise the apparent height of the fragments will be too large, and the calculated flattening ratio will be less than its true value. Outcrops suitable for study are not plentiful, for in addition to the

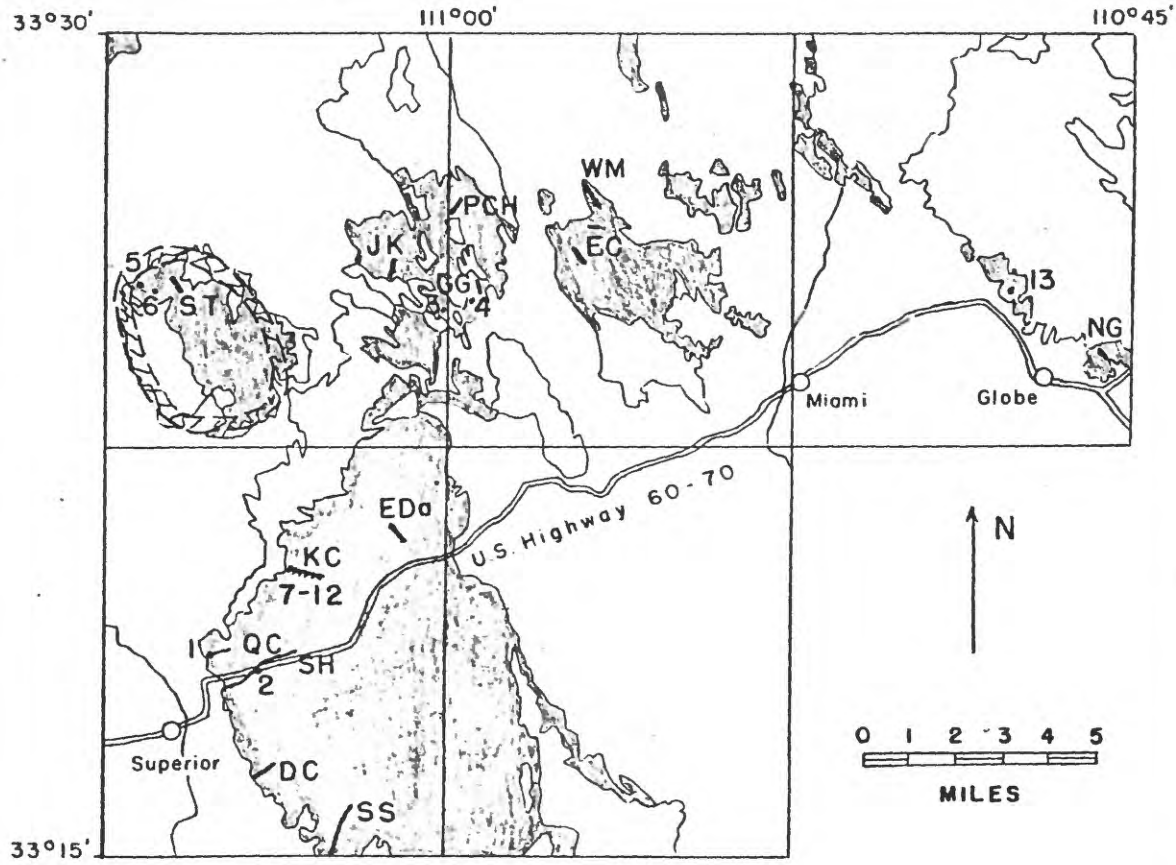

EXPLANATION

\ ST

Location of sections where flattening ratios and/or specific gravity were studied. Initials correspond to those of plates 2 and 3.

•4

Location of chemical analyses. Numbers correspond to specimens of table 6.

Dacitic ash flows

Other rocks

Approximate border of caldera.

Figure 19.--Map showing location of flattening ratio studies, specific gravity studies, chemical analyses, and approximate border of the caldera.

required near-vertical surface, the fragments must show a clear contrast with the matrix. Although most outcrops above the horizon of extreme flattening reveal pumice fragments, relatively few reveal them clearly enough for reasonably accurate measurements. An optimum degree of weathering on the surface is required; fragments may be completely obscured on some weathered surfaces, and on others they have been weathered away to leave small pits. In some places the pits are suitable for measurements, but in other places weathering has enlarged the pits beyond the original dimensions of the fragments. Another difficulty may be encountered in the white zone on little-weathered surfaces of fresh road cuts and excavations. Here the fragments cannot be seen clearly enough until a moderate amount of weathering has darkened the matrix.

Inferences derived from the flattening curves

As the slope of most of the curves of plate 2 is nearly uniform, the downward increase of flattening must depend on the constantly increasing factor of the weight of the overlying material. The greater the amount of overlying material, the greater will be the flattening. The steady, uninterrupted increase in flattening on most of the curves suggests that the entire mass was deposited in a relatively short time. The writer formerly thought that this progressive flattening indicated a single huge eruption for the entire ash-flow sheet (Peterson, 1959). Distinctly layered structures in some areas (figure 20) and a local reversal in flattening suggest eruptions as separate pulses, but the pulses followed one another closely enough for the sheet to comprise a

Figure 20.—Layered structure in the middle distance suggests that ash flows erupted in separate pulses. View is eastward across Devils Canyon near south edge of Superior quadrangle.

single cooling unit. If the underlying material had cooled to rigidity, it would have remained nearly undeformed by successive eruptions. If an earlier eruption had reached a condition sufficiently rigid to resist deformation, the underlying fragments would be less deformed, and the flattening curve would show a reversal. Below the break, such a curve could be expected to resume its gradual downward slope. A partial example of this type is curve EDa. Apparently the fragments at EDa 3 had more resistance to deformation than those at EDa 4, probably because they were cooler. This suggests a long enough time interval between successive eruptions to allow some cooling. As the break in the curve is small, it is likely that the time interval was short. A local reversal in zoning and specific gravity data also indicate a slight break in deposition in the vicinity of section EDa. The appearance of this break is shown in figures 21 and 22.

The curves of plate 2 are roughly parallel to one another. This shows that the flattening increases downward at about the same rate at different places, and implies similar physical conditions within the sheet over a wide area immediately after its eruption.

The amount of flattening of the pumice fragments is a particularly useful measure of the degree of welding of the tuff, because so much of the original groundmass texture has been obscured by later crystallization. We may assume that the more the pumice fragments have been flattened, the more intense was the welding. If this is a valid assumption, welding intensity increased downward until the pumice fragments became so thin that they cannot be detected at all.

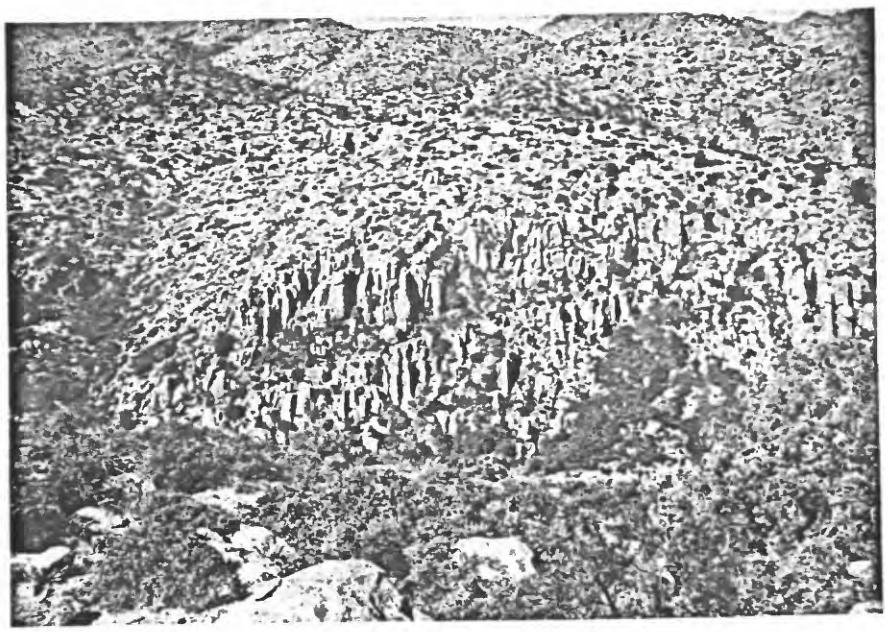

Figure 21.—Upward anomalous change from white zone to gray zone, Devils Canyon 1½ miles north of U. S. highway 60-70, Superior quadrangle.

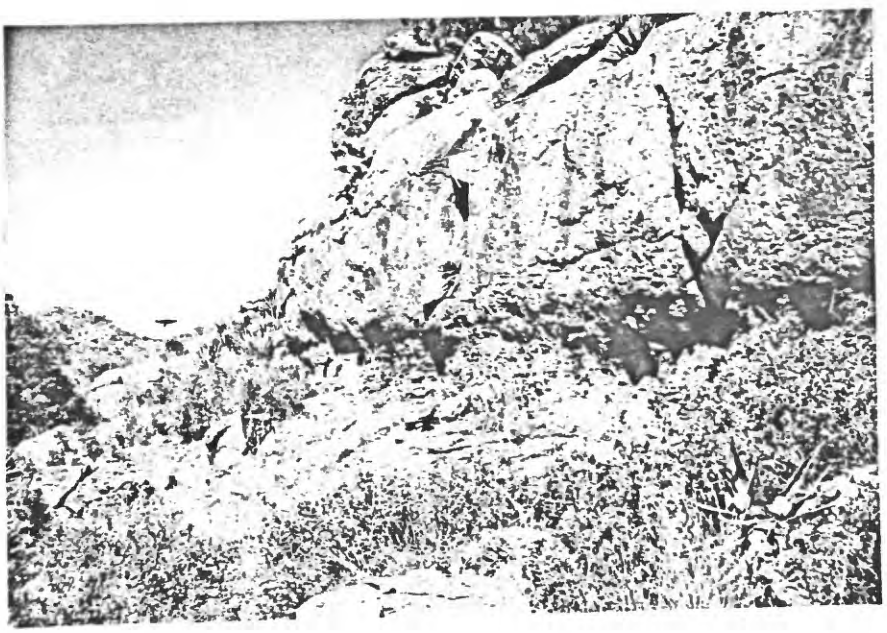

Figure 22.—Resistant bluff of gray zone rocks above softer rock of white zone. This shows the anomalous zoning reversal near Devils Canyon 1 to 2 miles north of U. S. highway 60-70, Superior quadrangle.

This condition is represented, for example, just below point 5Ha7 on curve SH. The tuff lying below this point was "densely" welded--the original pore space was nearly all eliminated by compression. The tuff lying above this point shows various degrees of partial welding. The curves of plate 2 show, for this deposit, that dense welding was not attained until materials were buried from 500 to over 1,000 feet. Many deposits are described in the literature, however, where dense welding is attained under much smaller thicknesses, presumably because the materials were hotter (Smith, 1960, p. 823-824).

The consistency of the flattening curves has certain practical applications. For example, an abrupt change in the amount of flattening between adjacent outcrops suggests that a fault passes between the outcrops, and this has proved to be one of the few criteria by which faults can be identified within the ash-flow sheet. Furthermore, from the average flattening ratios on opposite sides of a fault, an appropriate curve in plate 2 will show the approximate relative stratigraphic level of each of the points, and thereby the amount of throw on the fault can be estimated.

If the flattening ratio at a locality can be determined, it indicates the approximate stratigraphic level of the locality, even where erosion has deeply dissected the sheet. By projecting the curves of plate 2 upward, it might be supposed that the flattening ratios could be used to determine the original thickness of the sheet. Any such determinations would need to be regarded with caution, however, because: (1) Many pumice fragments were not originally equidimensional,

and these would have a tendency to land with their longer dimensions horizontal. Near the top of the deposit, therefore, the dimensions of the fragments do not necessarily give a true representation of the amount of flattening. (2) The physical environment at the top of the sheet is totally different from the well-insulated, near-uniform conditions lower down, so near the top the flattening curves may not maintain the consistent behavior that they exhibit in the lower part of the sheet.

The only curve in plate 2 that approaches the original top of the deposit, section SH, shows distinct irregularities near the top. This shows that thickness determinations by upward projection of the flattening curves are only approximate. If the curves were arbitrarily projected in a straight line to the point where the flattening ratio is one, the errors introduced would probably be similar at different localities, so the estimated total thicknesses would be approximately correct relative to one another. The flattening ratios, therefore, provide a means which in future studies may permit determinations of approximate original thickness of the sheet at certain appropriate points.

Specific gravity

Specific gravity studies of ash-flow sheets

An important criterion in the recognition of ash-flow deposits is the characteristic variation of specific gravity and porosity according to distance above the base. In his study of the New Zealand ignimbrites, Marshall observed a progressive decrease in specific

gravity from the base upwards and recognized that this decrease illustrated that the amounts of compaction and welding were at least in part a function of the amount of overlying material. He cited figures showing the relation between specific gravity and distance above the base (Marshall, 1935, p. 339, 350-351). Gilbert showed that the bulk specific gravity of the Bishop tuff decreased progressively from the bottom upwards (Gilbert, 1938, p. 1843). Erlows (1955, p. 1220-1221) showed similar variations for the welded tuff at Chiricahua National Monument, Arizona. In each of these examples, the porosity increases as specific gravity decreases. Composite diagrams showing the relations of specific gravity and porosity to the distance above the base for each of these deposits have been presented by Smith (1960, p. 826-827).

N. P. Peterson made some preliminary studies of specific gravity variations in the dacitic ash-flow sheet near Miami, Arizona, on specimens from Webster Gulch (N. P. Peterson, in press (1)). He found that upward from the base the specific gravity increases through the basal tuff to a maximum value in the vitrophyre, and that farther upward in the lithic dacite the specific gravity remains constant. He noted this was a departure from typical welded tuff bodies, and this helped support his conclusion that the dacitic body is of a different type than welded tuff deposits described previously.

Procedure used for studying specific gravity

Specific gravity was studied to determine both its vertical and lateral variations. The locations of measured specimens are shown

on the map of figure 19. Plate 3 shows the bulk specific gravity of each specimen and its stratigraphic distance from the base.

The bulk specific gravity of each specimen was measured on a simple beam gravity balance. The specimen was successively balanced in air and then in water, and its distance from the fulcrum at each balancing was used to calculate the specific gravity. Repeated determinations on single specimens showed reproducibility to about ± 0.02 units, and determinations on different specimens from the same locality were generally accurate to within ± 0.03 units. Determinations were less accurate on the porous rocks, because as soon as immersed the specimen begins to absorb water and the apparent weight continually increases. This error was partly offset by loose surface material sloughing off during immersion. However, after some practice on the apparatus an approximate balance could be obtained almost immediately after immersion of the specimen. Other possible sources of error would be from xenoliths of appreciably different specific gravity, and from possible vugs inside a specimen. More refined methods were not used because of the need to make a large number of determinations. Moreover, the results are thought to be easily accurate enough for the purpose of this study.

Porosity

Gilbert (1938, p. 1842-43), Enlows (1955, p. 1220-21), and N. P. Peterson (in press (1)) determined the porosity as well as the specific gravity of their specimens. The powder densities of the rocks submitted for chemical analysis were determined by the Denver Rock Analysis Laboratory of the U. S. Geological Survey, and these are

shown in table 1. If both powder density and bulk specific gravity of a rock are known, its porosity can be calculated, for the porosity bears a simple inverse relation to the bulk specific gravity. The three curves of figure 23 show the relation of porosity to bulk specific gravity based on the maximum, minimum, and mean rock powder densities of table 1. If a proper value is selected for the powder density, the porosity of a specimen can be determined from figure 23.

Variations of specific gravity

Plate 3 shows how specific gravity varies according to the vertical distance of specimens above the base of the sheet. A separate curve is shown for each section. Since different sections have different thicknesses of non-welded tuff at the base, the lowermost completely welded vitrophyre was arbitrarily selected as the origin for the vertical scale, and distances are shown both above and below the zero horizon.

In a typical section, with nonwelded tuff exposed at the base, the specific gravity increases upward to the vitrophyre; this agrees with N. P. Peterson's observations (p. 55). This upward increase in specific gravity appears at the base of sections QC, PCH, CG, MG, KC, and DC. A similar increase in specific gravity was also recorded by Marshall (1935, p. 339) in one of the New Zealand sections and by Enlows (1955, p. 1220) in one of the Chiricahua sections. Progressing upward, each of the specific gravity curves of plate 3 has a somewhat different shape, but the curves have certain general similarities. In sections where the total thickness exceeds about 600 feet, the specific gravity remains nearly constant with only minor variations, until close

Table 1. Powder densities and porosities of analyzed rock specimens. The percent porosity of each specimen is determined from the powder density and the bulk specific gravity.

Specimen	Zone	Powder density	Bulk specific gravity	Percent porosity
1. QCb5	vitrophyre	2.49	2.45	1.6
2. SHa10	gray	2.65	2.52	4.9
3. PCd1	vitrophyre	2.50	2.43	2.8
4. QCc3	gray	2.59	2.48	3.5
5. STb10	vitrophyre	2.48	2.44	1.6
6. STd2	brown	2.64	2.47	6.7
7. KC1	tuff	2.38	2.00	16.0
8. KC3	vitrophyre	2.49	2.48	0.4
9. KC9	brown	2.56	2.48	3.1
10. KC11	gray	2.52	2.42	4.0
11. KC12	white	2.54	2.34	7.9
12. KC13	pumice fragment	2.53	2.21	14.5
	Mean powder density:	2.53		

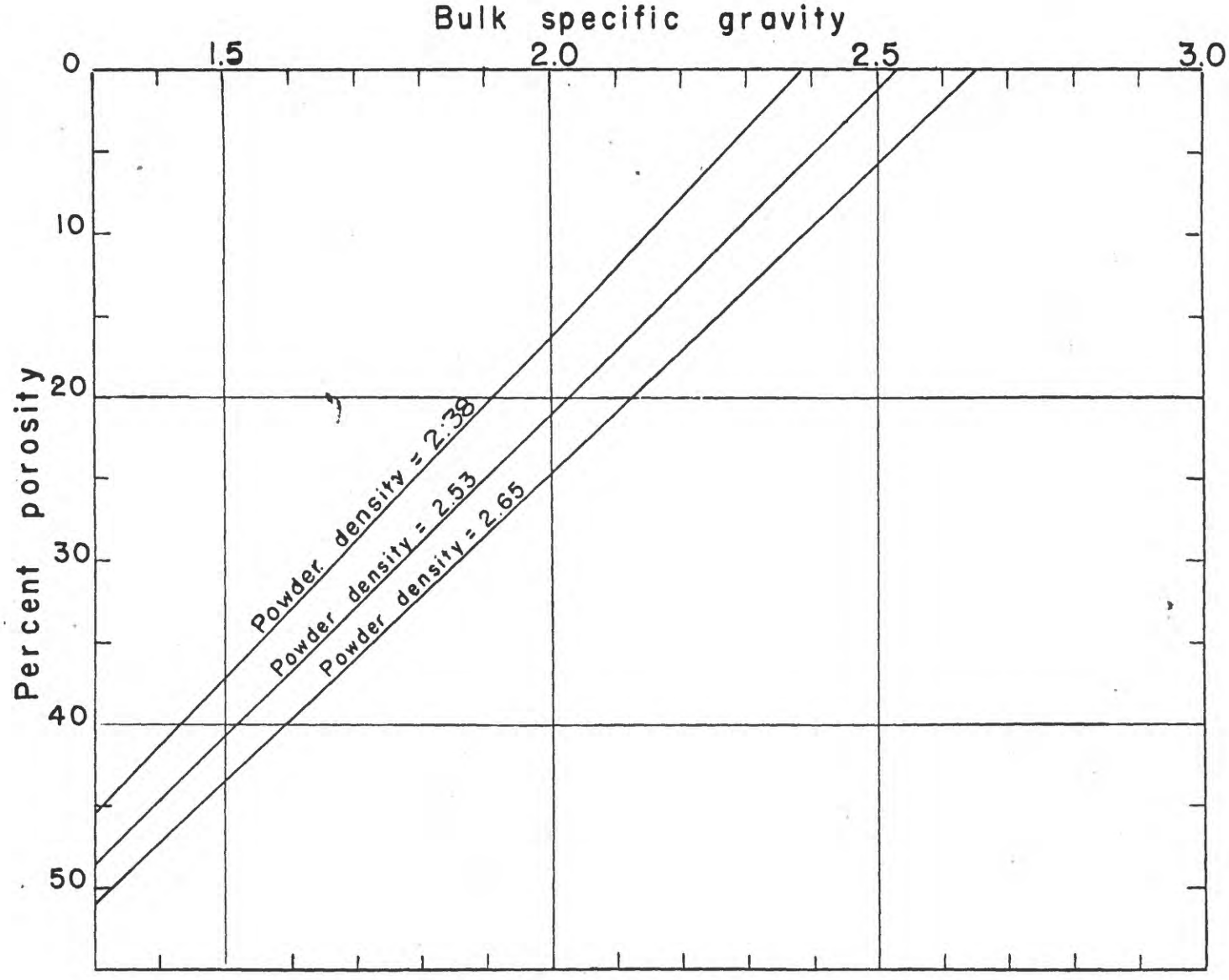

Figure 23.-- Relation of porosity to bulk specific gravity for powder densities of 2.38, 2.53, and 2.65.

to the top it begins a progressive decrease. In some of the thinner sections, such as JK and HQ, the specific gravity begins to decrease right above the vitrophyre. In most of the curves, the decrease at the top is consistent, and though some curves show a slightly erratic pattern, in all but EDa the decline is generally persistent.

At the base, the lowest value of specific gravity recorded was 1.8, and the specific gravity increases upward to between 2.40 and 2.45 in the vitrophyre. In some sections the specific gravity continues to increase upward above the vitrophyre to reach values of 2.50 to 2.54 in the brown and gray zones. In sections ST and SH the specific gravity remains close to 2.5 for over 1,000 feet. In other thick sections, such as QC, KC, DC, WM, and PCH the specific gravity persists above 2.4 to nearly the top of the section. The upward decline in specific gravity begins as much as 500 feet below the apparent top of the section, as in section SH. This relation could not be checked in most sections because the true top of the ash flow is either unknown or uncertain. The specific gravity declines from 2.4 or 2.5 to a minimum of about 2.1 or 2.2.

The minor fluctuations of specific gravity on the vertical part of the curves are probably not significant, reflecting only the inaccuracies of the procedure. It is possible, however, that more rigorously selected samples, spaced closer together in the sections might reveal minor but significant variations. The abrupt upward increase of specific gravity between specimens EDa4 and EDa5 is accompanied in the field by a local upward change from a white groundmass

to a gray groundmass (figures 21 and 22), and a nearby reversal in the pumice fragment flattening ratio (plate 2, section EDa). Together these data suggest a local interruption in deposition.

Inferences derived from the study of specific gravity

The most important conclusion from the specific gravity study is that the variations of specific gravity indicate the major part of the ash-flow sheet comprised a single cooling unit. If any part of the sheet had cooled appreciably before the following eruption was deposited, its upper part would show a decline in specific gravity, followed upwards by an abrupt increase, as in curve EDa. If successive eruptions had been separated by such time, sawtooth curves of the type shown for section EDa would be characteristic throughout the entire ash-flow sheet, but curves of the type of QC, PCH, and KC can be obtained only if the ash-flow sheet cooled as a single unit.

The increase of specific gravity downward from the top must have been caused by the increasing weight of overlying materials. At the point where the specific gravity reaches a constant value, close to its maximum, it is probable that the degree of compaction was maximum, that the porosity was very small, and that welding was complete. These characteristics persisted nearly to the base, where rapid chilling caused a progressive downward increase in particle rigidity accompanied by a decrease in the amount of compaction and welding.

The increasing compression with depth and the chilling at the base can explain the successive specific gravity decline at both the top and the base of the deposit, but can they alone explain the thick

zone of constant specific gravity? A comparison of the specific gravity curves (plate 3) with the flattening ratio curves (plate 2) suggests that the zone of maximum welding is much more restricted than is the zone of maximum specific gravity. This comparison shows that pumice fragments continue to be progressively flattened far lower in the sheet than the point where specific gravity reaches its maximum. What is the explanation of this apparent paradox?

It is likely that the degree of deformation of the pumice fragments represents at least in a general way the amount of deformation in the finer ash of the groundmass. Although there is probably a considerable differential in the absolute amount of deformation between fragments and particles of different sizes, the relative amounts of compression and welding are probably roughly equivalent. Therefore, where pumice fragments are only slightly flattened, the finer particles comprising the groundmass are probably only partly welded, even though the bulk specific gravity is maximum. Let us visualize the conditions in this zone right after eruption. Immediately after the emplacement, compression, and welding of the mass, the porosity was probably still relatively high in this zone, and the bulk specific gravity was correspondingly low. As cooling progressed, the glassy matrix crystallized, and other crystals were deposited by vapors in the pore spaces. Because the deposit was thick, cooling was slow, and crystals continued to grow in the pore spaces until, in this zone, the pores were completely filled.

In many ash-flow sheets the reduction of porosity is a direct

function of the degree of welding, and maximum specific gravity indicates complete welding. Because crystal growth during cooling was a major factor in reducing the porosity of this deposit, the specific gravity variations provide only supplementary information, and the degree of welding must here be determined mainly from the textural evidence.

The minimum specific gravity values of 2.1 or 2.2 at the top of the sheet are considerably higher than the minimum values of 1.3 to 1.8 reported from the tops of ash-flow sheets in New Zealand (Marshall, 1935, p. 339), near Bishop, California (Gilbert, 1938, p. 1843), and at Chiricahua National Monument, Arizona (Enlows, 1955, p. 1220). Besides removal of the former top by erosion, crystal growth in pore spaces is very likely a major reason for the abnormally high minimum value in this deposit. In New Zealand and at Bishop, an appreciable proportion of the groundmass is still glassy, whereas here it is entirely devitrified, and sanidine and cristobalite, the chief products of devitrification, have a higher specific gravity than the original glass.

Structure of the ash-flow sheet

Faults

The dacite in the vicinity of Superior, Miami, and Globe, Arizona is essentially a sheet-like deposit. The rock was laid down on a surface of considerable relief. The attitude of the layering varies from horizontal to dips up to about 30°; in a few places the dips are steeper. In several places throughout the area, early workers

recognized post-dacite faults which offset the edges of the dacite body. Before the present study, however, faults were not traced away from the borders because of the seemingly uniform lithology.

The zoning of the ash-flow sheet and the systematic changes in flattening ratios permitted faults to be recognized and mapped during this study. Because weathered surfaces of different zones have nearly a uniform appearance, the mapping was difficult and slow, and only a sample area was completed in detail. This detailed area lies in the northeast and central parts of the Superior quadrangle and is shown on plate 4. For this detailed study the ash-flow sheet was divided into 3 units. The lowermost unit includes the basal tuff, the vitrophyre, and the brown zone. The middle unit represents the gray zone, and the upper unit represents the white zone. Because the contacts between the three zones are gradational, the lines could be drawn only approximately; however, this located several faults with large displacements. Plate 4 shows that the faults are principally north-south trending, with their west side downdropped. The faults can be recognized by abrupt changes of groundmass color on freshly broken outcrops. Weathered surfaces commonly appear the same on both sides; only in a few places can faults be recognized from changes visible on weathered outcrops. In scattered localities fault zones are marked by brecciation and slickensides, and in some places faults identified first from lithologic evidence could be confirmed by well exposed fault zones.

A special symbol on the map of plate 4 shows the average flattening ratio of pumice fragments on opposite sides of some of the

faults at selected localities, and another symbol indicates approximate vertical separation on the faults. Structure sections on plate 5 illustrate that on each of the major north-south faults the west side is downdropped. This is the same sense of movement as that on the Concentrator fault, the major fault that lies along the base of Apache Loop.

Many smaller faults transect the ash-flow sheet, but it has not been possible to map them in the time available. Detailed work on these minor faults would be difficult because with decreasing displacement the lithologic differences on opposite sides of a fault become less distinct. Other large faults cut the ash-flow sheet outside the area mapped in detail, and a study of these structures would be an important contribution to understanding the tectonic history of the region.

Joints

Nearly everywhere the ash flows are cut by a system of vertical or near vertical joints (figures 2, 20, 21). They vary from clearly defined to indistinct, and from widely to closely spaced. Generally the joints are from 5 to 15 feet apart, but they may range from a few inches to more than 40 feet apart. They commonly form distinct joint systems, in which parallel joints extend continuously for several hundred feet to over a mile. In many places two joint systems intersect each other at angles from 60 to 90 degrees. The continuity of the joints suggests that instead of being simple cooling cracks, they are of tectonic origin. The joints might have developed during the cooling of the mass, but their directions were still controlled by stresses

imposed by regional tectonic activity. Polygonal cooling joints are found in a few places, mainly in the vitrophyre zone (figures 3, 7). The present study has included but little work on the joints, but a detailed study of the joints would undoubtedly be helpful in reaching a better understanding of the structural history of the area.

Source of the ash flows

Williams (1941) demonstrated that the close of extensive ash-flow eruptions is often marked by large-scale crustal collapse at the source to form calderas. Smith (1960, p. 817-820), who summarized the available information on source areas of ash flows, listed the major types of source areas as domes, craters, fissures, calderas, and volcano-tectonic depressions. He correlated the different types and sizes of ash flows with the information available on their source areas, and he concluded that the source areas of ash-flow deposits with volumes of more than a few cubic miles almost invariably show subsidence structures. This implies that either calderas or volcano-tectonic depressions now mark the sources of most large ash-flow deposits.

The ash-flow deposit of this study, containing at least 40 cubic miles or 165 cubic kilometers, falls in the range of magnitude order 6 on Smith's volume scale (1960, p. 819), which suggests that it issued from either a caldera or volcano-tectonic depression. As the deposit is probable mid-Tertiary, any topographic evidence of a depression due to subsidence after eruption has very likely been eroded away. The mapped area has been examined for possible evidence indicating subsidence at the time of eruption. Geologic relations in the southwest

part of the Haunted Canyon quadrangle suggest that this area may be occupied by the roots of a caldera. Its approximate boundary is outlined on figure 19 (p. 47). The detailed geologic features have been mapped by the writer (Peterson, 1960), and this map and report are included here as plate 6. Evidence suggesting a caldera can be summarized as follows: (1) relations among older rocks around the edge of the proposed caldera are complex and jumbled; (2) dacite shows intrusive relations into older rocks within and along the edge of the caldera in a few places; (3) older rocks are strongly brecciated adjacent to the caldera; (4) large broken blocks of older rocks lie in the volcanic rock near the border; (5) an unusually large number of lithic inclusions are locally found in the dacite within the caldera; (6) dacite and earlier volcanic rocks are locally altered within the caldera; (7) relative proportions of phenocrysts of rocks within the caldera resemble proportions in the rocks of the white zone more closely than those of the lower zones.

The border zone that contains most of the evidence forms a nearly circular ring 3 to 3½ miles in diameter in the southwest quarter of the map of plate 6. On Sawtooth Ridge about 1 mile west of the Kennedy Ranch, all the outcrops of diabase and Paleozoic and Apache group sedimentary rocks are highly brecciated. It is likely that some of the older rocks were engulfed by the volcanic rocks, and some of the contacts indicated as faults are actually intrusive. Proceeding southeastward clock-wise around the caldera border, across Rock Creek to a point due east of Bull Basin, diabase and Paleozoic sedimentary

rocks continue to be considerably brecciated, and the various rock formations bear complex and abnormal relations to each other. Irregular dike- and sill-like bodies of dacite transect the jumbled older rocks. The complete heterogeneity of bedding attitudes and fault patterns, and the probable intrusive relations of small dacite bodies in older rocks agree with the view that these rocks were involved with the collapse of a caldera.

Dacite is the only rock that crops out from the area east of Bull Basin to the southeast flank of Government Hill, at which point brecciated blocks of Escabrosa limestone and earlier volcanic rocks are surrounded by dacite. The dacite above these blocks is firmly welded and lithified instead of showing the usual basal zone of nonwelded tuff grading upward to vitrophyre. The contacts at the sides and base of the blocks are covered by brush and talus, but the relations as far as they are exposed suggest engulfment of the blocks during a caldera collapse.

From this point a fault that drops dacite against the older rocks can be traced southward for about a mile. The adjacent diabase and Paleozoic sediments are considerably brecciated. Southwest of Tony Ranch, the fault bends and continues in a west-southwesterly direction for about one-half mile before losing its identity in volcanic rocks. Continuing clock-wise around the caldera, the border zone between this point and the head of Haunted Canyon consists of complex, apparently intrusive relations between altered dacite, altered rhyolite, and quartz monzonite intrusions, and a thoroughly

shattered and brecciated block, about a mile in diameter, of diabase and Apache group rocks. This block is locally transected by dacite dikes, which in a few places are well exposed and exhibit distinctly intrusive relations.

From the point north of the divide between Haunted Canyon and Wood Camp Canyon, the border of the proposed caldera bends northwestward. The rocks along the border consist of brecciated and faulted Apache group rocks and diabase intruded by quartz monzonite porphyry. The rocks within the caldera are the earlier volcanic rocks and consist of considerably altered rhyolites and tuffs. A mile or so to the northwest, there is a series of nearly vertically dipping and overturned Apache group rocks which are relatively unfaulted and unbrecciated but dip steeply toward the caldera. As this is the only place in the entire area that vertically dipping sedimentary rocks were seen, and as the bedding strikes parallel to the border of the caldera, it is probable that the attitude was caused by the collapse of the caldera. These beds strike northwestward and the outcrops continue for about a mile. Beyond this point the edge of the caldera is marked by sheared and brecciated diabase and early Precambrian igneous rocks. The border of the caldera bends to extend nearly northward, and continues until it again crosses Sawtooth Ridge. The older rocks along the border are sheared, brecciated, and locally altered. The earlier volcanic rocks on Sawtooth Ridge consist mainly of altered rhyolite, and in a few places viscous plugs have possibly intruded indistinctly layered flows and tuffs. The border of the caldera bends to the northeast and

extends parallel to Sawtooth Ridge, probably along its northern flank. The older rocks along this border consist of extremely faulted and brecciated Main granite, diabase, and Apache group and Paleozoic sedimentary rock. Some units consist only of brecciated blocks and fragments. Other smaller totally brecciated units have been included with the earlier volcanic rocks on the map.

The deformation in this area is extraordinarily complex, possibly because the northeast-trending Kennedy fault intersects the border of the caldera in this area. It is not known whether or not the caldera collapse and the Kennedy fault are contemporaneous; however, it is likely that much or all of the movement on the Kennedy fault occurred after the eruption of the ash flows. This is because the dacitic sheet within the caldera southeast of the fault is quite thick, whereas no ash flows are found within several miles of the fault on the northwest side. Only in the extreme northwest corner of the Haunted Canyon quadrangle is the ash-flow sheet again encountered. It is reasonable to presume that the sheet once covered the intervening area, but due to the uplift of the block northwest of the Kennedy fault the dacite has been stripped away.

Much of the dacite within the boundary of the proposed caldera has a somewhat different appearance from the dacite of other areas. Megascopically, the groundmass appears to be partly bleached. Under the microscope, it can be seen that considerable clay and calcite have formed in the groundmass, and that feldspar, particularly plagioclase, has been partly altered to clay and calcite. This suggests that

mild hydrothermal alteration is the cause of the distinctive appearance of the rock. Alteration effects would be expected in a source area, so their presence within the proposed caldera and their absence elsewhere provide support for the view that this site was an eruptive source of the ash-flow sheet. Efforts to map alteration zones within this area were not successful, because transitions from altered to unaltered rocks are broadly gradational, and on weathered surfaces even the most altered rocks do not contrast distinctly with unaltered rocks. The modal analyses of rocks within the proposed caldera are slightly but distinctly different from most of the dacite from other areas. Briefly, the modes from the dacite within the caldera correspond most closely with the modes from the upper part of the sheet in outlying areas (see the section on Petrography). This suggests that the rock within the proposed caldera is closer to the mineralogical composition of the rocks erupted last in the dacite series, which is compatible with the view that the caldera is a source area for the dacitic ash-flow sheet.

A comparison of the volume of the ash-flow sheet and the volume of the caldera suggests that a collapse of this caldera alone cannot account for more than a half or a quarter of the material comprising the ash-flow sheet. The maximum diameter of the caldera is about 3½ miles, and its area is roughly 10 square miles. If we assume an original volume for the deposit of 40 cubic miles, and if the volume of surface foundering must equal the volume of the deposit, 4 miles of vertical downward movement would be required. While there is no

indication of exactly how much the movement might have been, 4 miles is almost certainly excessive. We might reasonably assume, however, that the subsidence was one to two miles. This would account for a volume of 10 to 20 cubic miles of rock, and leave some 20 to 30 cubic miles unaccounted for.

Other possibilities might account for the remaining rock:

1. Other source areas may lie in the vicinity that have not yet been recognized. They might be concealed under either the ash-flow sheet or Gila conglomerate, or they might lie outside the area that has been mapped.

2. Less intense subsidence may be distributed throughout the area around the caldera. For example, part of the subsidence of the graben between the Kennedy and Gold Gulch faults (plate 6) may be due to withdrawal of volcanic material. The entire 40 cubic miles could be attributed to an average subsidence of one-half a mile over some 50 square miles of this graben plus an additional 1½ miles of subsidence of the caldera.

In summary, the geological evidence in the southwest part of the Haunted Canyon quadrangle suggests that a nearly circular area collapsed to form a caldera, and that the adjacent rocks were brecciated, intricately faulted, and locally engulfed by volcanic magmas. Such a collapse may have been caused by the eruption of large amounts of volcanic materials from an underlying magma chamber, and the caldera may thus represent the source of at least part of the dacitic ash-flow sheet of the Superior-Globe-Miami area.

PETROGRAPHY AND MINERALOGY

Phenocrysts

The nature, distribution, and appearance of the phenocrysts throughout most of the ash-flow sheet are remarkably constant. The phenocrysts are nearly uniformly distributed, and they comprise from 35 to 45 percent of the rock. Plagioclase is the most abundant phenocryst mineral, followed by lesser amounts of quartz, biotite, sanidine, and magnetite. Hornblende is present in some specimens and absent in others. Sphene, apatite, and zircon are common accessories, and a few specimens contain a little tourmaline. The relative proportions of different kinds of phenocrysts vary only slightly from one zone to another and from place to place. The major phenocrysts generally average between one-half and 1 mm in diameter, and a few are as large as 3 mm.

A high proportion of phenocrysts in all zones of the sheet show broken faces, and tiny angular crystal fragments are scattered through the matrix. The fragmental appearance is not so obvious under medium and high power, nor is it particularly noteworthy in most hand specimens, but it stands out strongly under the low power of the microscope. The broken grains indicate that the constituents of the rock were violently disrupted during some stage of their development. Such grains are common in pyroclastic rocks but rare in lava flows.

Plagioclase

Plagioclase is the major phenocryst through the entire ash-flow sheet. Crystals are generally subhedral and rarely euhedral. All plagioclase grains are twinned, and most are twinned after two or three twin laws. Albite, Carlsbad, and pericline are the most common, and Manebach, acline, and ala twins have also been recognized. Most plagioclase phenocrysts are distinctly zoned, and may show either normal or oscillatory patterns.

Efforts during the present study to determine the position of the plagioclase in the albite-anorthite series have not led to a certain answer. Determination of plagioclase composition, particularly in volcanic rocks, is no longer a simple matter of determination of extinction angles. Recent studies of the plagioclase series have shown that the optical properties depend not only on the position in the albite-anorthite series, but also on the structural state of the crystal lattice, which in turn depends on the rate of cooling during and after crystallization, certain events in the thermal history of the rock, and possible ionic substitutions in the plagioclase lattice (Köhler, 1941; Tuttle and Bowen, 1950; Goodyear and Duffin, 1954; J. V. Smith, 1956; J. R. Smith and Yoder, 1956; MacKenzie, 1957; J. V. Smith and Gay, 1958). The ordered state of the crystal lattice is the low-temperature form of the mineral; it is found in plagioclase of plutonic bodies and the large gabbro complexes and represents long, slow cooling. The disordered state of the crystal lattice is the high-temperature form; it is found in synthetic plagioclase and a few

volcanic rocks and represents rapid cooling. The plagioclase of most volcanic and hypabyssal rocks has a structural state intermediate between complete order and disorder. The widely-used extinction angle curves were derived for low-temperature plagioclase; furthermore, they were drawn by averaging points that may show considerable spread. As the plagioclase of this study is from a volcanic rock, it doubtlessly represents an intermediate- or high-temperature form. Therefore the An-content as given from extinction angle curves is likely to be in error.

Despite the uncertain results, extinction angles of plagioclase in thin section have been measured both on the ordinary microscope stage and the universal stage. Quick, routine determinations were made on most slides, and more detailed studies of several slides were made on the universal stage. No appreciable variations were noted from one rock sample to another. Reasonably consistent values of An-content were generally obtained, though a few determinations on complex twins deviated considerably from the bulk of the results. According to extinction angle curves, most plagioclase grains, including zoned crystals, fall in the composition range An 35-40. A few grains have centers as calcic as An 55, and some of their borders may reach An_{25}. Such wide variations are rare, however, and very few crystals show a range of more than about 10 percent An, centered about the interval An_{35-40}.

Perhaps one of the more reliable methods of plagioclase determination is from the indices of refraction but even this is subject to

errors. J. V. Smith and Gay (1958, p. 759) indicate that the An-content is but an estimate, as the standard curves have been obtained by averaging refractive indices of analyzed plagioclases. They point out that the variations of refractive index with the structural state have not been systematically studied, but cite other work that has shown appreciable variation in refractive index from the ordered to disordered state for sodic plagioclase. They think that the refractive index is not much affected by the structural state in calcic plagioclase.

In this study the high and low refractive indices of cleavage fragments of plagioclase have been determined in immersion oils, and the plagioclase composition has been estimated from Tsuboi's curves (Winchell, 1951, p. 280). The determinations have been made on specimens KCl, 3, 9, 11, 12, and 13. Because of zoning, the refractive indices have a considerable range. However, for most grains lying on 001, the fast ray has a refractive index of 1.539-1.540, and the slow ray 1.547-1.548. Tsuboi's curves indicate a plagioclase composition of about An_{22-25} for these values. The minimum fast ray index observed was 1.534, equivalent to An_{14}, and the maximum slow ray index seen was 1.551, which for a grain lying on 010 would be An_{38}. No variation in average refractive index was noted from one rock specimen to another. It is likely that zoning extended over a wider range than was observed in this refractive index study. We may conclude that the average composition and the extreme ranges of plagioclase indicated by refractive index are considerably more sodic than those indicated by extinction angles. This plagioclase is probably sodic enough for the refractive

index to be affected by the change in the structural state, so the indicated An-content must be regarded as uncertain. However, even if the maximum error of 5 percent is allowed (Smith and Gay, 1958, p. 759), the An-content determined from refractive index is considerably more sodic than that determined from the extinction angles. This deviation shows that these data are not sufficient to yield a definite position or range of position of the plagioclase on the albite-anorthite scale.

Supplemental information can be provided from X-ray diffraction studies, but still a unique solution cannot be obtained. J. V. Smith and Gay (1958, p. 749, 754) have derived curves from which either An-content or structural state can be determined if the other is known. Although neither is known precisely, the optical studies have roughly indicated the composition, so the approximate structural state of the plagioclase can be deduced.

Figure 24 shows X-ray diffraction records of plagioclase phenocrysts from specimens KC1, 3, 9, 11, 12, and 13. Table 2 gives the recorded values of 2θ for the crystal faces $(\bar{2}01)$, $(1\bar{1}1)$, (220), $(1\bar{3}1)$, and (131), and the values of B (capital beta) and Γ (capital gamma) as defined by J. V. Smith and Gay (1958, p. 748, 749, 754). Figure 25 reproduces the curves of Smith and Gay showing the relation of B and Γ to An-content. Each value of B and Γ is plotted on figure 25 against two assumed values of An-content; An_{22} yielded by refractive index, and An_{38} yielded by extinction angles from low-temperature curves. Although both points are probably in error, the true An-content probably lies somewhere nearby. For B the range of uncertainty is too wide to permit

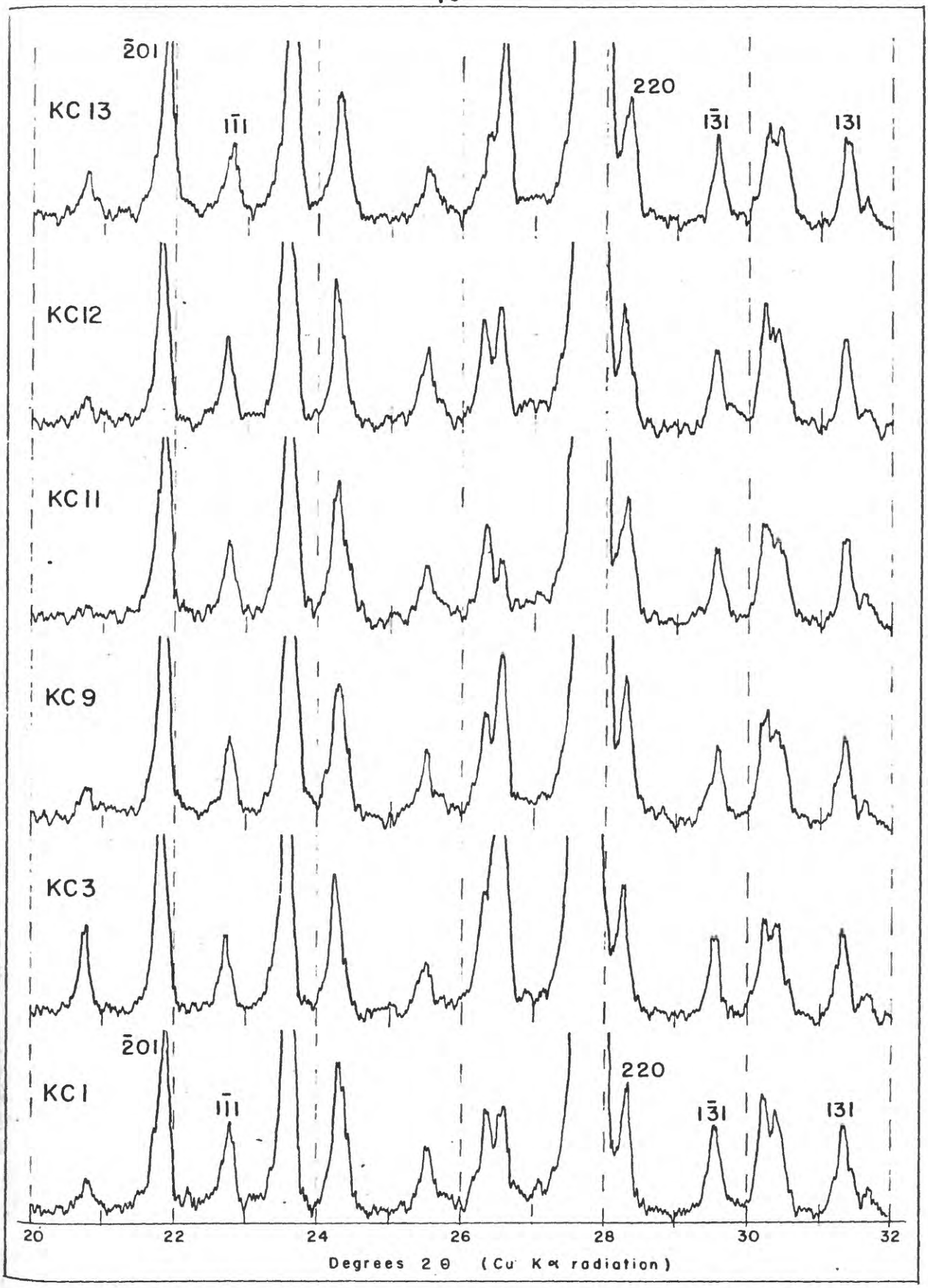

Figure 24.-- X-ray diffraction patterns of plagioclase phenocrysts.

Table 2. Plagioclase 2θ

	2θ of $(1\bar{1}1)$	2θ of $(\bar{2}01)$	B	2θ of (131)	2θ of (220)	2θ of $(1\bar{3}1)$	Γ
KC1	22.81	21.92	.89	31.40	28.27	29.57	.53
KC3	22.77	21.93	.84	31.33	28.28	29.55	.51
KC9	22.82	21.92	.90	31.38	28.35	29.61	.51
KC11	22.75	21.87	.85	31.32	28.28	29.54	.52
KC12	22.77	21.85	.92	31.31	28.28	29.52	.55
KC13	22.87	21.96	.89	31.43	28.37	29.65	.50

B = 2θ of $(1\bar{1}1)$ - 2θ of $(\bar{2}01)$

Γ = 2θ of (131) + 2θ of (220) - 4θ of $(1\bar{3}1)$

any useful conclusions, as it extends all the way from the low to the high temperature curve. The range is narrower for Γ, however, as the points fall midway between the low and high temperature curves. This confirms the suggestion that this plagioclase, from a volcanic rock, has partly ordered and partly disordered lattice structure.

Sanidine

Most of the ash-flow sheet contains only a small percentage of sanidine phenocrysts. The phenocrysts are subhedral or euhedral, but broken faces are common, and some grains show slight corrosion and embayment of their borders. The grains are untwinned, show uniform extinction, and are nowhere altered.

X-ray diffraction methods were used to estimate the Or-Ab content of the sanidine, and the results are shown in table 3. Bowen and Tuttle (1950) have shown that the peak for the reflection $\bar{2}01$ changes position according to relative amounts of the K- and Na-feldspar, and Donnay and Donnay (1952) and Orville (1958) have provided additional data. Figure 26 shows partial X-ray patterns of sanidine and accompanying quartz from two different specimens.

The curve of Bowen and Tuttle (1950, p. 493) shows composition as a function of the absolute spacing of the $\bar{2}01$ planes, whereas the curve of Orville (1958, p. 208) shows composition as a function of the 2θ difference between the $\bar{2}01$ peak of sanidine and the 101 peak of $KBrO_3$. As quartz was a persistent contaminant of these samples, and as the 101 peak of $KBrO_3$ is masked by the 100 peak of quartz, the determination was modified here to use quartz as a standard and

Table 3. Determination of sanidine composition from data of Tuttle and Bowen (1950) and Orville (1958)

	2θ of sanidine $\bar{2}01$ peak read on chart	2θ of quartz 100 peak read on chart (standard=20.862)	Corrected 2θ of sanidine $\bar{2}01$ peak	Spacing of $\bar{2}01$ planes	Sanidine composition from Bowen & Tuttle (1950)	Corrected 2θ of sanidine $\bar{2}01$ minus 2θ of $KBrO_3$ 101 (20.205°±.010)	Sanidine composition from Orville (1958)
KC9	20.98	20.75	21.09	4.2124 Å	Or88-Ab12	0.88	Or85-Ab15
KC12	21.070	20.827	21.105	4.2094 Å	Or89-Ab11	0.900	Or84-Ab16

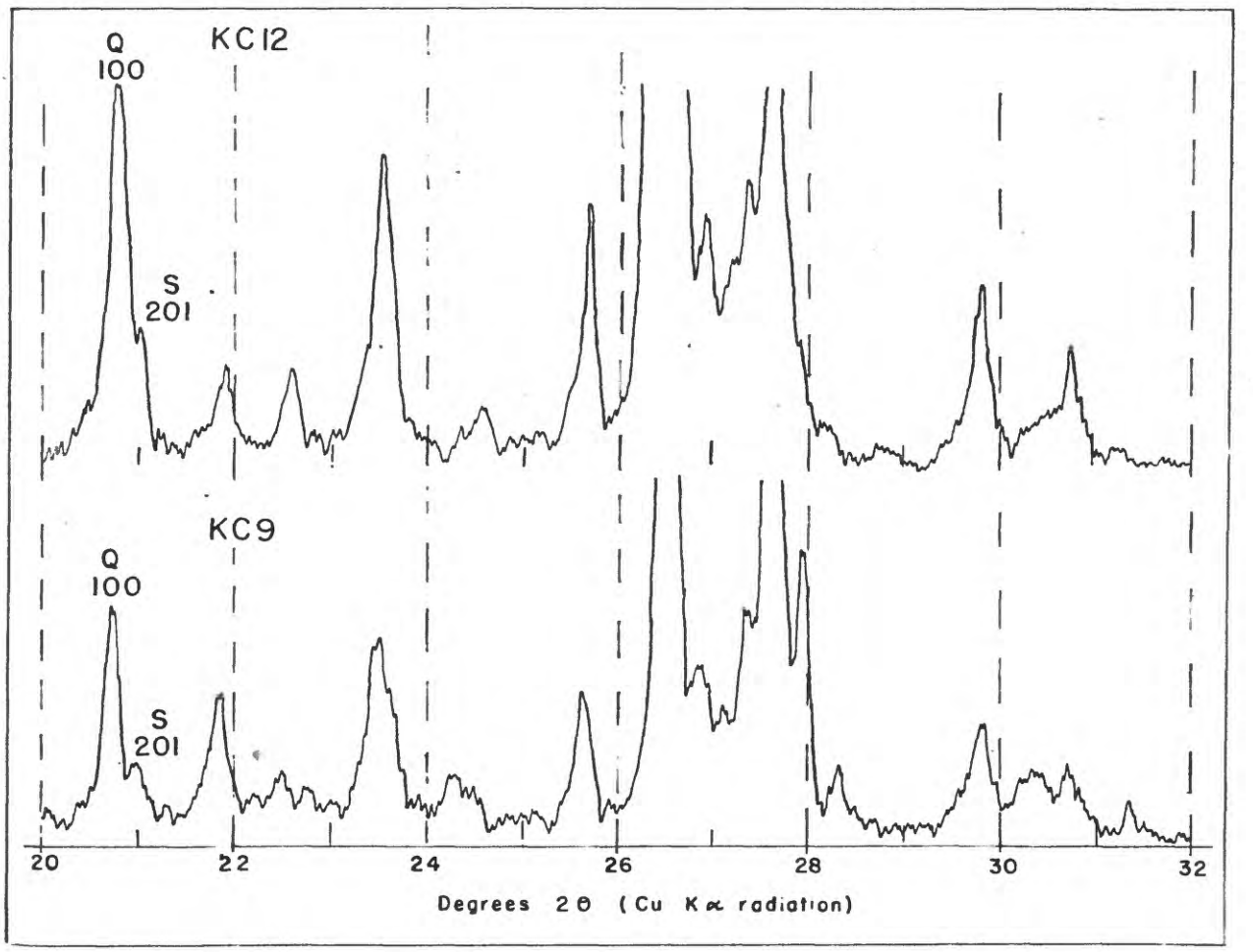

Figure 26 -- X-ray diffraction patterns of sanidine phenacrysts. Quartz and cristobalite are also present in samples.

correct the 2θ value of the 100 peak to its standard value of 20.862° Cu Kα radiation. Because of these modifications of technique, a high degree of precision is not claimed for these determinations. However, the determinations are reasonably consistent, and we may conclude that the sanidine composition lies in the approximate range of Or_{84}-Ab_{16} to Or_{89}-Ab_{11}.

Quartz

Quartz phenocrysts are anhedral and approximately equant, and they generally have deeply embayed borders. Broken faces are common, and tiny fragments of quartz are fairly abundantly scattered through the groundmass. Grains are clear and unaltered, and some have tiny liquid or vapor inclusions. In most specimens the quartz shows slightly undulatory extinction.

Biotite

Biotite phenocrysts are generally euhedral or subhedral, and form tabular books and flakes. Borders are generally sharp, but some grains show frayed edges at the ends of cleavage traces. Many grains are distorted and bent. "Bird's-eye" structure typically causes non-uniform extinction. Common inclusions are primary opaque oxides and tiny euhedral apatite grains. Properties of fresh biotite from rock specimen KC_3 are: $\beta \cong \gamma \cong 1.635 \pm .003$; 2V about 15°; pleochroism is pronounced with X = yellow, Y = Z = dark brown.

Biotite from the lower part of the ash-flow sheet shows no sign of alteration, but in the upper part of the brown zone the biotite

shows slight alteration, and upward the alteration becomes progressively more intense. The first signs of alteration are bleaching at grain borders and development of small clots of opaque oxides in the bleached areas. In more intensely altered grains, bleaching progresses inward, particularly along cleavage planes, and the opaque grains increase in size and concentration. In the gray zone, some of the biotite is partly altered to chlorite, but much of it is lighter colored biotite. Alteration in the white zone is moderate to extreme, and in some rock specimens biotite is considerably bleached and nearly opaque from the crowded clots of oxide; in some other specimens it is partly to largely altered to chlorite, and in a few specimens only a shell of opaque oxide grains indicates the former presence of biotite.

Basal tuff

The tuff at the base of the ash flow is typically a nonwelded vitric crystal tuff, with phenocrysts set in a vitroclastic matrix. The texture of the basal tuff is unmistakably pyroclastic; thin sections show cuspate and lunate glass shards interspersed with fine dust. Figure 27 illustrates the texture of the basal tuff.

In the lower part of the tuff, shards are undeformed and randomly oriented, but upward they show a tendency to become squeezed and flattened. This tendency marks the transition between the basal tuff and the vitrophyre.

The shards and ash fragments that comprise the matrix of the tuff are glassy and isotropic. The index of refraction of the glass ranges from 1.496 to 1.499. Some shards and fragments show dim

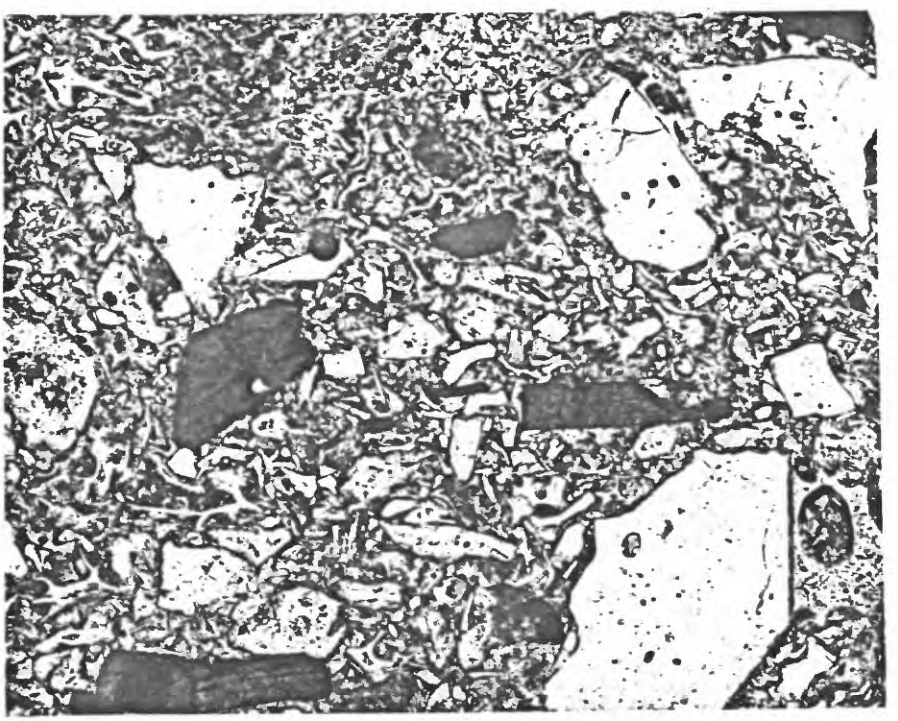

Figure 27.—Undeformed and nonwelded, typically vitroclastic texture of the basal tuff, specimen 402. Photograph by Elliot C. Morris.

birefringence, indicating slight devitrification. A preliminary X-ray study suggests that the matrix contains K-feldspar, cristobalite, and a zeolite mineral, probably clinoptilolite. All the phenocrysts in the tuff are fresh.

Vitrophyre

The vitrophyre zone consists of highly welded vitric crystal tuff, with phenocrysts set in a completely glassy groundmass. Although megascopically much of the glass appears massive and uniform, under the microscope the glass is typically seen to consist of individual shards and fragments that have been flattened, distorted, and tightly welded together. Under medium and high power, the vitrophyre commonly exhibits textures that are characteristic of the welded tuffs described in the early, widely known papers of Marshall (1935), Mansfield and Ross (1935), and Gilbert (1938). In the vitrophyre these typical textures are readily identified, but in parts of the overlying zones they have been partly to completely obscured by devitrification and crystallization.

In most of the vitrophyre the groundmass consists of two separate types of glass that show varying amounts of contrast with each other. One type comprises the shards and lapilli, and the other comprises the intervening matrix. The glass of the shards and lapilli is typically clear, and contains little or no dust or crystalline fragments. Its color in plane light ranges from colorless to light and medium brown. Color of this glass within a single specimen is generally uniform, but the color varies widely from one field location to another. The glass of the matrix is generally cloudy in

appearance, contains moderate to large amounts of dusty material, and is highly charged with small, broken crystalline fragments. Under medium and high power it can be seen that the glass itself is colorless, but dust commonly imparts an apparent brown or grey color. In some specimens the borders of the shards and lapilli are sharp and contrast distinctly with the matrix, but in others the borders are vague and the shards and lapilli tend to merge into the matrix. The tiny crystal fragments impart an apparent low birefringence to the matrix, whereas the shards and lapilli remain completely isotropic. This difference helps to distinguish the shards and lapilli from the matrix, especially in specimens in which borders are vague.

Figure 28 shows typical textures of the vitrophyre. Highly deformed shards are abundant in the center of the photograph, and are common through the whole field of view; they show a wide variety of distorted shapes. The clear, brown glass of the shards stands out distinctly from the light-colored, dust-charged glass of the intervening matrix. The matrix of this specimen contains only a moderate amount of dust and is relatively clean.

Brown zone

The brown zone, like the vitrophyre, is composed of highly welded tuff, but instead of a glassy groundmass its phenocrysts lie in a cryptocrystalline and microcrystalline groundmass. Original textures are generally preserved, and in the microscope the highly flattened and deformed shards and lapilli are readily seen to be tightly welded together. Crystallization has been superimposed on the primary

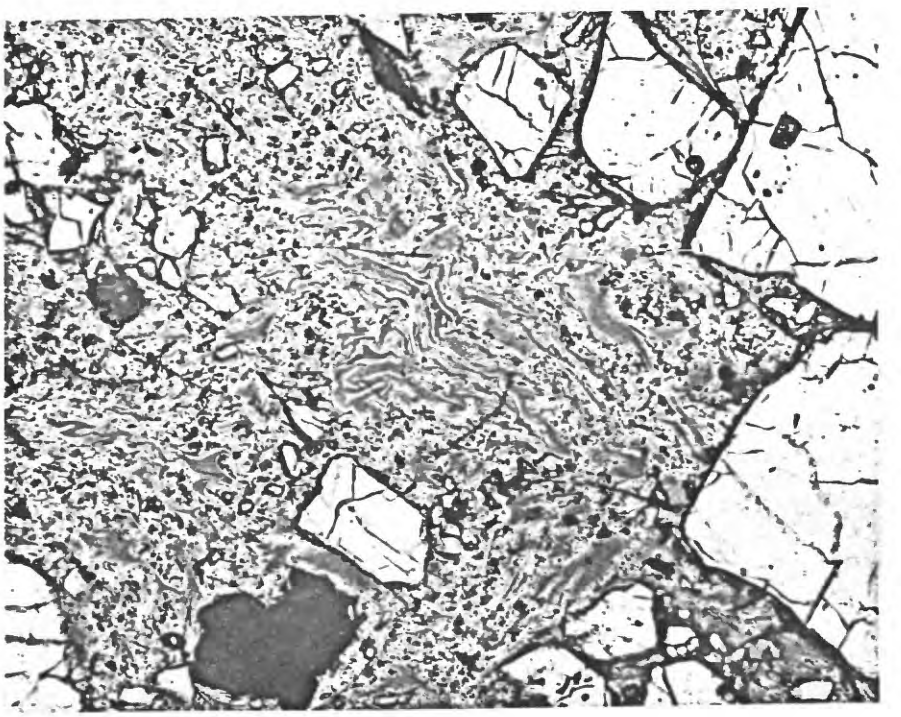

Figure 28.—Tightly welded tuff of the vitrophyre, showing highly deformed textures. Specimen QCb5. Photograph by Elliot C. Morris.

welded textures, and the brown zone is equivalent to Smith's zone of devitrification (Smith, 1960, p. 831).

Under the microscope, the minerals comprising the crystallized groundmass could be only tentatively identified as silica minerals and feldspar. On the X-ray spectrometer, however, the groundmass was found to contain mainly cristobalite and K-feldspar, and subordinate amounts of quartz and plagioclase.

The primary textures of most individual specimens closely resemble those described for vitrophyre; the principal difference is that the vitrophyre groundmass is glass, whereas the groundmass of the brown zone is generally cryptocrystalline. In the vitrophyre, distinct glass phases distinguish shards and lapilli from the matrix, and in the brown zone each of the two phases may show an individual character of crystallization by which they may be distinguished. In the shards and lapilli, the crystallization is more prominent, as the crystals are generally larger than those in the intervening matrix. In some specimens an abrupt change in crystal size distinctly marks the borders of shards and lapilli. The borders of most shards and lapilli are formed of slender needles, probably of cristobalite and K-feldspar, arranged in spherulitic or axiolitic patterns. The individual needles range from 0.005 to about 0.05 mm in length. The interior parts of shards and lapilli are commonly intergrowths of tiny anhedral grains, approximately equidimensional, which form random patterns. Individual grains commonly range from barely discernible to 0.01 mm in diameter.

The matrix is generally less well crystallized than are the

shards and lapilli; in part of the matrix crystallization can be detected only as a faint birefringence, and individual crystals cannot be distinguished. In most areas, however, crystallization is distinctly visible as low birefringent aggregates and scattered spherulitic growths, probably mainly of cristobalite and K-feldspar. A fine brown dust pervades most of the matrix. The dust is locally concentrated in lenticular, sinuous, and irregular bands, layers, and masses, and these concentrations reflect and sometimes emphasize the textural relations between shards and lapilli and the matrix. The dust is probably iron oxide, but it could not be positively identified because X-ray patterns of the groundmass showed no appropriate peaks.

In some specimens the crystals of the groundmass reach about 0.2 to 0.3 mm in diameter, and the intergrowths have granophyric texture. Quartz is the dominant mineral in the coarser grained intergrowths, accompanied by K-feldspar and a little plagioclase. It is not known whether these coarser intergrowths developed during the original cooling of the rock or subsequently. These textures may indicate a gradation to Smith's granophyric zone of crystallization (Smith, 1960, p. 831), and would presumably be caused by an unusually long period of cooling.

Variations among specimens from the brown zone are considerable. In some areas high concentrations of yellowish brown dust nearly obscure the primary eutaxitic texture. In some areas, even though the groundmass is lithoidal due to devitrification, the crystals are so small that the groundmass is nearly isotropic. In contrast, in many specimens the

crystallization of matrix and shards has progressed far enough so that their boundaries have been obscured, and a clear distinction between the two phases is not possible. Dust and broken phenocryst fragments are generally more abundant in the matrix than in the shards. In some specimens, however, dust and fragments have been mixed into the shards and lapilli, so the criterion of differential concentration of dust and fragments cannot be universally used to distinguish the phases.

In most specimens of the brown zone all the phenocrysts are entirely fresh. In the upper part of the zone, however, where the gradation between the brown and gray zone begins, biotite shows slight bleaching and development of opaque grains at its borders.

Gray zone

Rocks of the gray zone are welded crystal tuff, with phenocrysts set in a cryptocrystalline groundmass. Because the primary textures of the groundmass are partly to considerably obscured by crystallization, the degree of welding is not distinct. Interpretation of relict textures indicate, however, that the lower part of the zone is probably densely welded, and that within the zone the degree of welding decreases upward. The crystallization of the groundmass indicates that the gray zone is part of Smith's zone of devitrification, and it is likely that the upper part of the gray zone is grading into his zone of vapor phase crystallization.

X-ray spectrometer patterns again show that cristobalite and K-feldspar are the principal groundmass minerals, and that quartz and plagioclase are subordinate. In some thin sections, groundmass

crystals have grown large enough to permit visual confirmation of the X-ray data.

In at least some specimens in the gray zone, the two distinct phases of the primary texture can be distinguished by differential amounts of crystallization. Crystals in lapilli and shards are larger and more distinct; individual fibrous crystals of the spherulites and axiolites along the lapilli borders reach 0.1 mm in length, and the anhedral grains of their interiors are generally 0.001 to 0.02 mm in diameter. In general, the shards and lapilli are relatively free of dust and broken phenocryst fragments, though some mixing has occurred. In contrast, the crystals comprising the matrix are much smaller, generally up to 0.05 mm, and in some places the matrix is nearly isotropic.

The size of the groundmass crystals tends to increase upward in the gray zone, and in some specimens no difference in crystal size is apparent between lapilli and matrix. As the degree of crystallization increases, considerable interpenetration occurs between shards and lapilli and the matrix, and the boundaries of the lapilli and shards become more and more diffuse. In many specimens, particularly in the upper part of the gray zone, the outlines of the original shard-size fragments have been completely obliterated by crystallization, and the borders of the lapilli are so vague that they can be recognized only with difficulty. The matrix generally contains considerable amounts of broken phenocryst fragments, and this differential concentration of crystal fragments and dust may aid in distinguishing primary textures where they have been obscured by crystallization.

The matrix is generally cloudy from a high content of dust, probably hematite, which is differentially concentrated into billowing and waving bands and lenticles that flow and swirl around phenocrysts and closely resemble true flow structure (figure 29). Careful scrutiny over a larger field of view shows, however, that the flow lines are discontinuous and lenticular, and that many of them are concentrations along borders of flattened lapilli. Lapilli range from a few mm to several cm in length, and if thin sections are cut through large lapilli, flow lines defined by dust concentrations may extend across an entire thin section. Unless microscopic observations are carefully correlated with close megascopic examination, it would be easy to conclude erroneously that this texture was developed in a lava flow. The obscuring of original pyroclastic texture by crystallization and the apparent flow structure imparted by dust concentrations, such as are seen in figure 29, are probably the principal reasons that the dacite sheet was not earlier identified as being of ash-flow origin.

Quartz, plagioclase, and sanidine phenocrysts remain unaltered throughout the gray zone. Biotite tends to be fresh in the lower part, but upward it shows progressively greater amounts of alteration. In figure 29 the biotite is considerably altered.

Microscopic examination has not revealed any obvious reason for the difference in megascopic appearance between the rocks of the brown and the gray zone. No consistent color difference in the groundmass dust was noted under the microscope, but it is possible that changes of environment at different levels in the cooling unit could

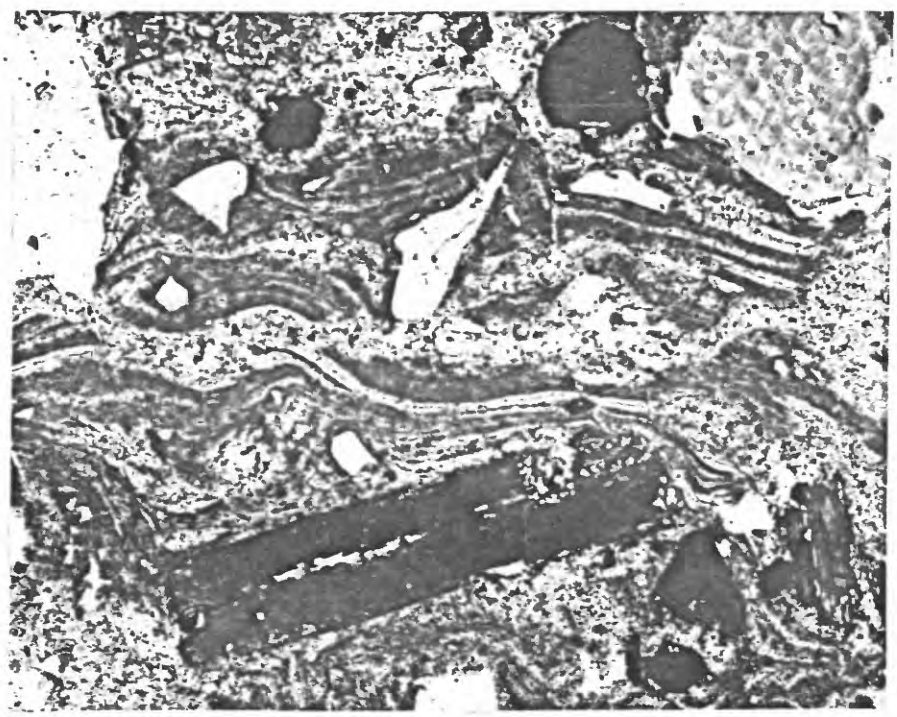

Figure 29.—Microscopic textures in the gray zone. Original details of welded vitroclastic textures have been obscured by devitrification, and differential dust concentrations along flattened lapilli borders simulate fluidal flow structures. Biotite phenocrysts contain much opaque oxide as alteration product. Photograph by Elliot C. Morris.

cause actual differences in the composition of the dust that would show up as a bulk color change. Whether or not such a change occurs in the dust is not known, but it does seem likely that the combination of several textural features may effect gradual upward changes which produce the zonal distinction. Those factors having most effect are probably the upward increase in groundmass crystal size, the more diffuse borders of shards and lapilli, the upward decrease in intensity of welding, and the introduction of vapor phase crystallization.

White zone

The white zone is composed of partly welded to perhaps non-welded crystal tuff, with phenocrysts lying in a cryptocrystalline groundmass. The degree of welding must be mainly inferred, because the original groundmass textures are nearly all obliterated by crystallization. Both devitrification and vapor-phase crystallization have acted on the rocks of the white zone.

The groundmass minerals were identified under the microscope as silica minerals and feldspar. Some groundmass cristobalite and quartz can be discerned optically, and sporadic tridymite crystals are noted. However, the great bulk of the material in the groundmass can bear only generalized optical identification. Preliminary X-ray work revealed K-feldspar and cristobalite as dominant, quartz subordinate, and plagioclase as minor.

The groundmass of typical specimens from the white zone is entirely cryptocrystalline, and consists of scattered spherulites and masses of randomly crystallized material. Locally the spherulites are

closely crowded together and have mutually interfered with one another's growth, but in most places the groundmass texture is xenomorphic with a light sprinkling of spherulites. In some places relict textural features can be distinguished, generally vaguely defined lapilli up to several millimeters in diameter. In a few places relict outlines of small lapilli and shards down to 0.1 mm in length can be identified.

The spherulites are probably composed of K-feldspar and cristobalite. They generally range from 0.05 to 1 mm in diameter and rarely reach 2 mm. They generally consist simply of radiating fibrous crystals, and their borders may be either sharply or vaguely defined. A few show concentric structures superimposed on the radial pattern. An appreciable number form complete spheres, but many consist only of sectors of spheres.

The bulk of the groundmass is xenomorphic granular, consisting of tiny intergrown crystals of silica minerals and feldspar. In some places they are fibrous or rod-like, but generally the grains are anhedral and more or less equidimensional. Relict lapilli and shards may have a type of crystallization different from that of the matrix, that is, they may be coarser or finer than the matrix, have axiolitic borders, be crowded with tiny spherulites, or have some other distinctive crystallization pattern. Contrast between the crystallization textures show a great variety of combinations, and no consistent interrelations between the lapilli and matrix could be detected. Grayish brown dust is abundant in both the spherulites and the xenomorphic part

of the groundmass; generally only in the relict lapilli is the rock relatively free of dust. The dust is generally randomly scattered and only rarely is concentrated into flow-like bands as in the brown and gray zones.

Quartz, plagioclase, and sanidine phenocrysts remain essentially fresh in the white zone, though quartz tends to be more deeply embayed. Biotite, however, is moderately to nearly completely altered. Surprisingly, even in rocks with extremely altered biotite, the scattered hornblende phenocrysts remain fairly fresh. An appreciable number of phenocrysts of graphically intergrown quartz and sanidine have been noted in the white zone. At the present time only their presence is recorded, and no explanation for them is offered.

Proportions of phenocrysts and their variations

Modal analyses of some sixty thin sections of dacite have been made. Most of the analyses were made using the Chayes point counting method (Chayes, 1949), but a few were run on an integrating stage. Results of the analyses are shown in table 4. These results show that most of the ash-flow sheet has a nearly uniform distribution of phenocrysts, and that relative proportions of the phenocryst minerals to one another are fairly constant. The proportions of phenocrysts from dacite in the southwest part of the Haunted Canyon quadrangle, however, show a distinct and consistent difference from the phenocryst proportions in other areas. Also certain minor variations between zones are noted at some localities. To determine which of these differences are real and which are only apparent, the modes were averaged and the 95%

Table 4. *Modes of dacite specimens.* Phenocrysts are calculated to 100 percent. Table also shows proportions of phenocrysts and groundmass, number of points counted in each slide, and zone from which specimen was taken. Starred (*) specimens have chemical analyses

Specimen and Zone	Plagio-clase	Sani-dine	Quartz	Biotite	Magne-tite	Horn-blende	Acces-sories	Percent phenocrysts	Percent groundmass	Number of points
*QCb5 v	71.6	.5	9.2	9.1	5.3	4.1	tr	34.1	65.9	639
QCb10 g	73.2	1.5	10.2	12.1	1.5	.1	1.4	39.4	60.6	669
QCb17 g	72.5	1.0	10.6	9.1	3.1	2.5	1.2	38.4	61.6	1,349
SH4 g	75.4	1.3	8.5	10.7	1.9	1.9	.3	43.5	56.5	708
*SH3 g	72.9	4.4	14.6	5.8	2.0	tr	.3	44.7	55.3	768
(2 secs)	69.0	3.6	13.9	9.1	3.2	.3	.9	41.7	58.3	812
SH1b w	65.0	9.9	13.3	6.6	2.5	2.5	.2	42.4	57.6	1,220
*KC1 t	67.1	2.2	15.1	12.9	2.7	-	tr	30.6	69.4	1,194
KC2 t	77.1	1.4	9.0	8.6	2.8	1.1	tr	40.8	59.2	1,560
*KC3 v	70.9	.2	10.6	10.6	2.9	4.2	.6	39.1	60.9	1,328
KC4 t	71.9	2.1	12.6	6.8	4.2	2.4	tr	38.6	61.4	1,722
KC5 t	66.7	3.1	13.1	9.8	4.7	2.6	tr	36.8	63.2	1,661
KC6 v	73.4	1.0	7.8	11.0	3.2	3.6	tr	45.1	54.9	1,542
KC7 b	77.5	1.1	4.6	11.5	3.7	1.4	.2	42.7	57.3	1,277
KC8 b	78.3	2.9	5.6	5.4	4.2	3.6	tr	40.5	59.5	1,185
*KC9 b	77.0	.2	7.8	8.6	4.4	1.7	.3	35.4	64.6	1,669
KC10 b-g	79.1	1.0	4.8	8.8	3.6	2.7	tr	32.5	67.5	1,603
*KC11 g	73.2	2.8	11.0	9.6	2.3	1.1	tr	42.3	57.7	1,333
*KC12 w	68.7	4.2	16.4	5.8	2.1	2.2	.6	40.7	59.3	1,644
*KC13 pumice	62.8	6.9	20.4	7.8	1.6	.5	tr	37.6	62.4	1,630
D1a t	67.5	1.5	13.3	11.8	3.0	2.2	.7	32.3	67.7	418
D1b t	72.0	4.6	7.5	9.8	1.7	3.5	.9	38.0	62.0	910
D1c t	68.3	4.2	13.6	10.5	2.0	1.4	tr	41.8	58.2	845
D1d v	72.5	1.8	11.5	8.2	3.6	2.4	tr	44.8	55.2	739
D2 b	72.4	2.0	11.5	6.3	7.0	tr	.8	36.0	64.0	integrating stage
D3 g	68.0	3.3	12.6	12.4	3.0	.1	.6	40.5	59.5	
D4 g	67.6	10.9	10.6	6.8	3.5	tr	.6	44.5	55.5	
D5 g	66.5	3.8	13.8	8.7	6.6	tr	.6	38.6	61.4	
D6 w	67.6	6.9	12.5	6.1	5.6	.8	.5	39.8	60.2	

Table 4. (Continued)

Specimen and Zone		Plagioclase	Sanidine	Quartz	Biotite	Magnetite	Hornblende	Accessories	Percent phenocrysts	Percent groundmass	Number of points	
WM4	g	65.4	8.1	14.1	7.7	2.4	1.7	.6	34.0	66.0	1,371	
JKa2	g	71.6	2.6	11.9	8.4	3.8	1.5	.2	40.3	59.7	1,438	
NGb4	v	73.8	4.4	5.9	11.1	2.4	2.4	tr	36.0	64.0	1,647	
NGb7	b	70.1	2.3	12.5	10.9	2.6	1.6	tr	36.5	63.5	851	
CCa1	v	66.0	5.4	10.7	12.3	3.3	1.3	1.0	42.1	57.9	712	
CCa2	g	71.0	4.3	11.1	8.7	2.5	1.2	1.2	44.0	56.0	737	
GGb5	t	75.3	2.4	6.2	6.7	4.3	4.0	1.1	31.3	68.7		integrating stage
GGb7	v	69.4	1.3	10.9	10.0	3.3	4.2	.9	33.3	66.7		
GGb8	b	75.0	2.1	6.7	9.0	4.2	2.5	.7	36.8	63.2		
GGb11	b	79.1	.5	5.2	9.1	3.6	2.3	.2	33.3	66.7		
GGb12	b	73.4	2.0	9.3	8.4	5.7	1.1	tr	37.1	62.9		
*GCc3	g	72.3	2.7	13.4	8.3	2.1	---	1.2	46.3	53.7		
*PCd1	v	71.6	2.4	7.3	10.7	2.8	5.2	tr	35.8	64.2	807	
PCd2	b	80.1	1.1	6.8	9.0	3.0	---	tr	38.2	61.8	697	
PCd3	b	72.5	4.4	10.0	10.3	2.8	---	tr	39.7	60.3	810	
TP4	not identifiable	62.7	9.9	18.5	6.3	2.6	---	tr	38.8	61.2	1,195	
TP5		64.0	14.5	12.5	5.1	3.1	---	.8	40.2	59.8	636	
TP8		55.0	13.0	22.2	9.8	tr	---	tr	42.3	57.7	671	
TP22		61.5	11.9	12.7	9.7	4.0	---	.2	36.6	63.4	1,102	
TP25		58.8	10.1	19.8	10.1	.8	---	.4	39.0	61.0	685	
ST2		58.2	6.3	23.2	8.0	2.1	1.2	1.2	44.0	56.0		integrating stage
ST4		59.2	7.6	19.0	11.7	1.6	tr	.9	41.2	58.8		
ST5		63.5	9.9	16.4	6.3	2.5	tr	1.3	45.2	54.8		
ST7b		57.5	9.1	20.3	9.3	2.8	tr	1.0	43.5	56.5		
ST9		58.9	10.6	19.4	8.4	1.9	tr	.8	44.6	55.4		
ST10		57.2	10.8	24.0	5.6	1.0	tr	1.4	46.4	53.6		
ST12		60.1	7.7	19.7	6.9	4.1	1.3	.2	41.1	58.9		

Table 4. (Continued)

Specimen and Zone	Plagioclase	Sanidine	Quartz	Biotite	Magnetite	Hornblende	Accessories	Percent phenocrysts	Percent groundmass	Number of points
ST14 not	60.1	9.4	19.3	8.2	2.0	tr	1.0	42.6	57.4	
ST17 ident.	58.6	9.2	21.0	6.7	3.1	tr	1.4	43.2	56.8	
*STd2 b	59.2	11.9	16.8	9.2	1.9	tr	1.0	39.7	60.3	1,721
*STb10 v	58.9	12.5	17.4	8.7	1.7	.8	tr	28.2	71.8	855

confidence limits determined; a summary is presented in table 5. The table is graphically illustrated in the bar diagrams of figure 30, which is patterned after the diagrams of Meckin (1960) and Williams (1960). The confidence limits of some of the figures of table 5 are broad because the means are taken from only a few samples. More modal analyses are planned so that figures will be based on more samples, and perhaps the confidence limits will be improved.

The statistical study reveals that:

1. No significant difference has been revealed in the number of phenocrysts in the rocks from different zones or from different localities. Statistically, the phenocrysts are quite uniformly distributed through the entire sheet.

2. The relative proportions of plagioclase, sanidine, quartz, and hornblende are significantly different between dacite from the southwestern part of the Haunted Canyon quadrangle and the dacite from other areas. These differences are generalized as follows:

	Plagioclase	Sanidine	Quartz	Hornblende
Southwest Haunted Canyon quadrangle	59½	10	19	nil
Other areas (omitting white zone)	71-74	2-3½	9-12	1-3

No significant differences are noted in the proportions of biotite, magnetite, or minor accessories.

3. The differences in proportions of plagioclase, sanidine, and quartz among the basal tuff, vitrophyre, brown, and gray zones are probably not significant.

Table 5. Weighted means[1/] of modes of different zones of the ash-flow sheet, with 95% confidence limits

Zone	plagioclase	sanidine	quartz	biotite	magnetite	hornblende	phenocrysts	degrees of freedom of weighted sample
Tuff	73.9 ±10.1	2.4 ±2.5	8.9 ±6.6	8.7 ±5.0	3.0 ±3.0	2.5 ±3.6	36.5 ±12.0	2
Vitrophyre	71.15 ±2.10	2.13 ±1.56	9.24 ±1.70	10.38 ±1.07	3.38 ±.78	3.42 ±1.07	38.79 ±3.95	7
Brown	73.65 ±4.66	2.15 ±88	9.88 ±4.04	8.90 ±3.09	4.25 ±3.07	.90 ±1.67	36.80 ±2.39	3
Gray	71.35 ±2.18	3.52 ±1.45	11.92 ±.92	8.95 ±.58	2.88 ±1.02	.73 ±.67	42.73 ±2.25	5
White	67.10 ±4.72	7.00 ±7.08	14.07 ±5.12	6.17 ±1.01	3.40 ±4.77	1.83 ±2.26	40.97 ±3.28	2
South-western part of Haunted Canyon quad	59.63 ±1.36	10.13 ±1.18	18.99 ±1.84	8.09 ±1.05	2.23 ±.63	not measurable	41.89 ±1.50	14

1/Where more than one specimen is from one zone in a single area, the mean of their modes was determined first, and it was this mean that was used, along with those from other areas, to find the over-all mean of the zone which is shown in the table.

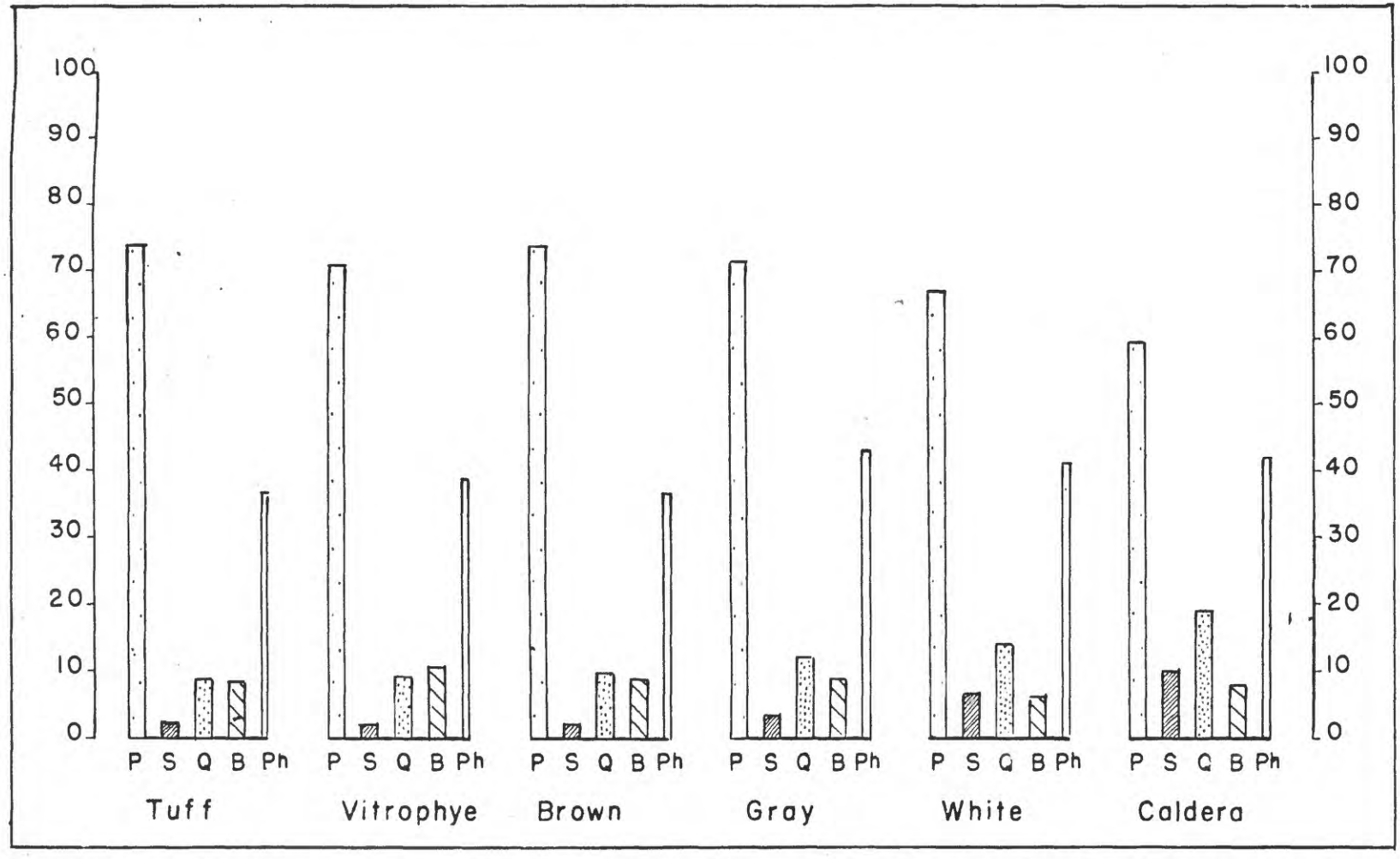

Figure 30.--Average proportions of plagioclase, sanidine, quartz, biotite, and the total phenocryst percentage for each zone and for the caldera.

4. The proportions of plagioclase, sanidine, and quartz of the white zone may be significantly different from the other zones, but more analyses are needed to narrow the confidence limits. It appears from present data that the proportions in the white zone are transitional between the rocks of the underlying zones and the rocks of the southwestern Haunted Canyon quadrangle.

These observations lead to the following conclusions:

1. The rock in the southwestern part of the Haunted Canyon has a significant difference in mineralogical composition from that in neighboring areas.

2. The rocks of the southwestern part of Haunted Canyon are closer in mineralogical composition to the rocks of the white zone than they are to the rocks of the lower zones.

These conclusions are compatible with the field and structural evidence for a source or vent area for the ash-flow sheet in the southwestern part of the Haunted Canyon quadrangle. If the composition of the magma being erupted from a vent were to change in a particular direction, we should expect (1) the rock occupying the vent at the close of activity to be different from the earliest rock erupted from the vent; and (2) the rocks in the vent to be closer in composition to the rocks that lie at the top of the volcanic series than to the earlier rocks that are lower in the volcanic series.

The changing phenocryst proportions, therefore, support the view that a source area for the dacitic ash-flow sheet occupies the southwestern part of the Haunted Canyon quadrangle.

CHEMISTRY

Table 6 gives twelve new chemical analyses of the dacite and the norms calculated from these analyses. Numbers 1 through 6 are standard rock analyses by Dorothy F. Powers and numbers 7 through 12 are rapid analyses by P. L. D. Elmore, S. D. Botts, I. H. Barlow, and G. Chloe. The location of each of the specimens is shown on figure 19 (p. 47). Numbers 1 through 6 are of pairs of specimens from three different localities: Queen Creek, Pinto Creek, and Sawtooth Ridge. Each pair has one specimen of vitrophyre and one specimen of lithic rock. Numbers 7 through 12 are from northeast of King's Crown Peak, and are a series of specimens consisting of the basal tuff, vitrophyre, brown zone, gray zone, white zone, and pumice fragments from the white zone. Number 13 is the analysis of dacite from near Globe given by Ransome (1903, p. 92-93, analyst, E. T. Allen).

A quick glance through the analyses and norms shows that in a general way the chemical composition of the specimens is nearly uniform. Except for specimen number 7, the basal tuff, which has been considerably altered, no appreciable differences among the specimens are readily apparent. Figure 31 shows a triangular plot of normative quartz, orthoclase, and albite plus anorthite for each of the thirteen analyses, and the grouping of points on this diagram emphasizes the uniform chemical composition. The similarities of chemical composition strongly support the view that the entire ash-flow sheet was formed

Table 6. Chemical analyses and norms of dacite

ical lyses	1 QCb5	2 SHa10	3 PCd1	4 QQc3	5 STb10	6 STd2
SiO_2	68.20	68.63	67.12	69.45	68.67	70.38
Al_2O_3	14.84	15.21	15.02	15.00	14.13	14.51
Fe_2O_3	1.95	2.80	2.39	2.67	1.34	2.22
	.73	.14	.54	.09	.94	.35
	.92	.80	1.15	.63	.83	.65
	2.20	2.43	2.58	2.12	2.23	1.81
O	3.71	3.89	3.70	3.93	3.71	3.78
	3.88	3.83	3.07	3.84	3.76	4.08
	.46	.79	1.15	.72	.79	.58
	2.06	.40	2.22	.57	2.73	.70
P_2O_5	.46	.50	.51	.47	.41	.44
	.00	.08	.00	.01	.00	.01
	.12	.13	.13	.12	.10	.11
	.08	.09	.07	.07	.08	.06
TAL	99.61	99.72	99.65	99.69	99.72	99.68
	26.16	25.38	26.76	27.12	27.00	28.50
	22.80	22.80	18.35	22.80	22.24	23.91
	31.44	33.01	31.44	33.01	31.44	31.96
	10.01	10.29	11.95	8.62	10.29	8.06
	.92	.82	1.12	1.22	.10	.92
	2.30	2.00	2.90	1.60	2.10	1.60
	1.12	2.88	1.92	2.72	1.86	2.24
	1.16		.70			
	.91	.46	.91	.30	.76	.91
	.34	.34	.34	.34	.34	.34
		.59		.78		

Table 6 (Cont'd)

7 KC-1	8 KC-3	9 KC-9	10 KC-11	11 KC-12	12 KC-13	13
66.4	67.8	67.7	68.0	68.7	69.8	68.76
14.4	15.3	16.3	16.5	16.7	16.0	15.48
2.1	2.1	2.5	2.6	2.7	2.2	2.50
.34	.77	.13	.12	.1	.1	.44
.80	.72	.76	.52	.38	.34	.56
2.3	2.3	2.5	2.4	2.2	1.9	2.23
1.8	4.0	4.1	4.2	4.2	4.0	3.89
4.3	3.6	3.6	3.5	3.6	4.0	3.88
7.1	2.3	1.8	1.8	1.4	1.3	.79 .57
.41	.46	.43	.40	.40	.36	.50
.05	.05	.05	.05	.05	.05	.00
.10	.14	.16	.14	.15	.12	.06
.09	.09	.08	.08	.08	.06	.02 .03 .03 .08
100	100	100	100	101	100	99.82
33.6	25.1	24.3	24.8	26.0	27.0	25.68
25.6	21.1	21.1	20.6	21.1	23.9	22.80
15.2	34.1	34.6	35.6	35.6	34.1	33.01
10.6	10.6	11.1	10.6	8.3	7.8	11.12
2.9	1.2	1.6	1.9	2.5	2.1	.82
2.0	1.8	1.9	1.3	1.0	.9	1.40
1.9	1.1	2.6	2.6	2.7	2.2	2.56
.2	1.4					
.8	.9	.5	.5	.3	.3	.91
.3	.3	.3	.3	.3	.3	
		.4	.4	.6	.6	

Table 6 (Cont'd)

Number	Field Number	Location
1.	QCb5	Vitrophyre, 1 mile northeast of Superior, Ariz.
2.	SHa10	Dacite, gray zone, 1½ miles northeast of Superior
3.	PCd1	Vitrophyre, 1 mile north of junction of Haunted Canyon with Pinto Creek, Haunted Canyon quadrangle
4.	GCc3	Dacite, gray zone, 1½ miles west-northwest of Porphyry Mountain, Inspiration quadrangle
5.	STb10	Vitrophyre, north side of Sawtooth Ridge, 0.7 miles southwest of BM 3677, Haunted Canyon quadrangle
6.	STd2	Dacite, brown zone, Sawtooth Ridge, 1.3 miles southeast of BM 3677, Haunted Canyon quadrangle
		Analyst for QCb5, SHa10, PCd1, GCc3, STb10, STd2: Dorothy F. Powers, Denver Rock Analysis Laboratory, U. S. Geological Survey
7.	KC1	Basal tuff, northeast of Kings Crown Peak, Superior quadrangle
8.	KC3	Vitrophyre, northeast of Kings Crown Peak, Superior quadrangle
9.	KC9	Dacite, brown zone, northeast of Kings Crown Peak, Superior quadrangle
10.	KC11	Dacite, gray zone, northeast of Kings Crown Peak, Superior quadrangle
11.	KC12	Dacite, white zone, northeast of Kings Crown Peak, Superior quadrangle
12.	KC13	Pumice fragments in white zone, northeast of Kings Crown Peak, Superior quadrangle
		Analysts for KC series: P. L. D. Elmore, S. D. Botts, I. H. Barlow, G. Chloe (Rapid rock analyses), U. S. Geological Survey
13.		"Biotite-dacite, one-fourth mile north of Old Dominion mine, Globe, Ariz.; E. T. Allen, analyst." (Ransome, 1903, p. 92-93).

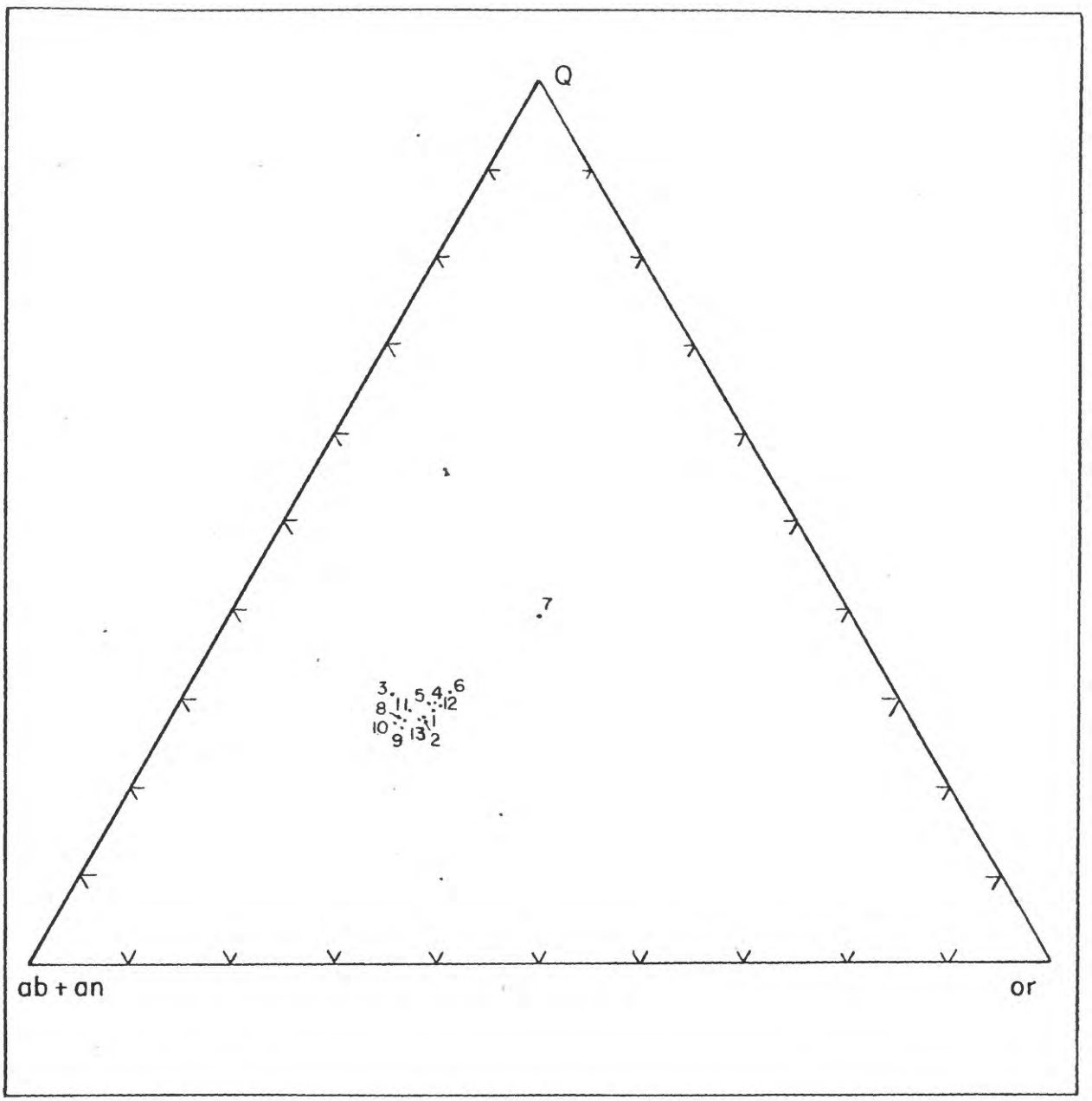

Figure 31.—Triangular plot of normative quartz, orthoclase, and albite plus anorthite for the thirteen analyses in table 6. Except for altered specimen number 7, the analyses cluster closely together, indicating nearly uniform chemical composition.

during a continuous series of eruptions and that it originated in a single magma chamber.

The analyses closely resemble the "average dellenite" as given by Nockolds (1954, p. 1014), and though they also lie close to his "average rhyodacite," in most respects they are closer to the dellenite. According to Rittmann's chemical scheme of classification (Rittmann, 1952, p. 93-102), all the rocks except number 3 fall in the field of "quartz-latite," and number 3 falls on the boundary between "quartz-latite" and rhyodacite (quartz latite and dellenite are commonly considered to be synonyms). These names contrast with the name dacite, which was established by megascopic and microscopic study of the phenocrysts. The difference merely illustrates that a high proportion of K-feldspar lies in the cryptocrystalline groundmass that is too fine-grained to be counted in a microscopic determination.

An attempt has been made to determine whether the small variations in chemical composition bear any relation to the position of the specimen in the ash-flow sheet. Data are probably too few to definitely establish possible relations, but a few of the slight changes seem consistent. Plate 7 is a variation diagram, with weight percent SiO_2 plotted against weight percent of each of the other important oxides. In specimens 1 to 6 a line connects each vitrophyre with its corresponding lithic specimen, and lines join the specimens of the series 7 to 12. The following observations seem pertinent:

1. Each of the lithic specimens 2, 4, and 6 has a higher SiO_2 content than its corresponding vitrophyre. In the series 7 to 12,

with one exception, SiO_2 progressively increases upward in the section.

2. Ferric iron is higher and ferrous iron and magnesium are lower in rocks from the upper part of the ash-flow sheet than they are in the vitrophyre.

3. Calcium generally declines upward in the sheet, but the decline is not consistent.

4. Potassium generally increases upward in the sheet, but the increase is not consistent.

Changes in aluminum and sodium are too small or too erratic to establish a trend.

The changes in ferric and ferrous iron are consistent with a view that rocks higher in the section had a greater opportunity to react with the atmosphere and therefore have a higher oxidation state.

The trends of SiO_2, CaO, MgO, and K_2O all indicate slightly greater differentiation in the rocks higher in the section that were erupted later. This trend is the reverse of what might be expected in the standard picture of an erupting magma chamber. Ordinarily, the upper, more highly differentiated and therefore more silicic and alkalic part of the magma erupts earliest, and comprises the lower part of the volcanic pile. The less differentiated magma, lower in the chamber, is less silicic and more calcic, and erupts later to form the upper part of the volcanic pile.

In this ash-flow sheet, the geologic evidence indicates that the eruption of the entire pile took place in a short time. To explain the reversed chemical trend, it is suggested that the chemical

composition of the erupting magma was essentially uniform, and that the slight changes in chemical composition were produced after eruption by the upward streaming of volatiles during the cooling of the mass.

Possible depth of origin

The depth of origin of the dacite magma may be estimated from the experimentally determined equilibrium crystallization diagram of Tuttle and Bowen (Bowen, 1954, p. 10; Tuttle and Bowen, 1958, p. 75). The diagram is reproduced in figure 32, and is the "equilibrium crystallization diagram for mixtures of albite, orthoclase, and quartz showing position of boundary curve between the fields of quartz and feldspar at various pressures of water vapor indicated in atmospheres on each curve. The cross bar on each curve indicates the position of the minimum temperature for that curve (pressure)." (Bowen, 1954, p. 10.)

Normative Q, or, and ab for each analysis of table 6 (except altered specimen 7) have been recalculated to 100% and plotted on the diagram. The points cluster near the cross bars that indicate minimum temperature, and fall between the 2,000- and 4,000-atmosphere curves. If we postulate that the total rock pressure is equivalent to water vapor pressure, we may conclude that the magma was developed by selective melting under a rock pressure of 2,000 to 4,000 atmospheres, which indicates a depth of 6½ to 13 kilometers (assuming an average rock density of 3). This depth should be regarded as only approximate, for several factors may affect the determination in unknown ways. It is not known, for example, what error is introduced by assuming the water vapor pressure equal to the rock pressure. The chemical composition of

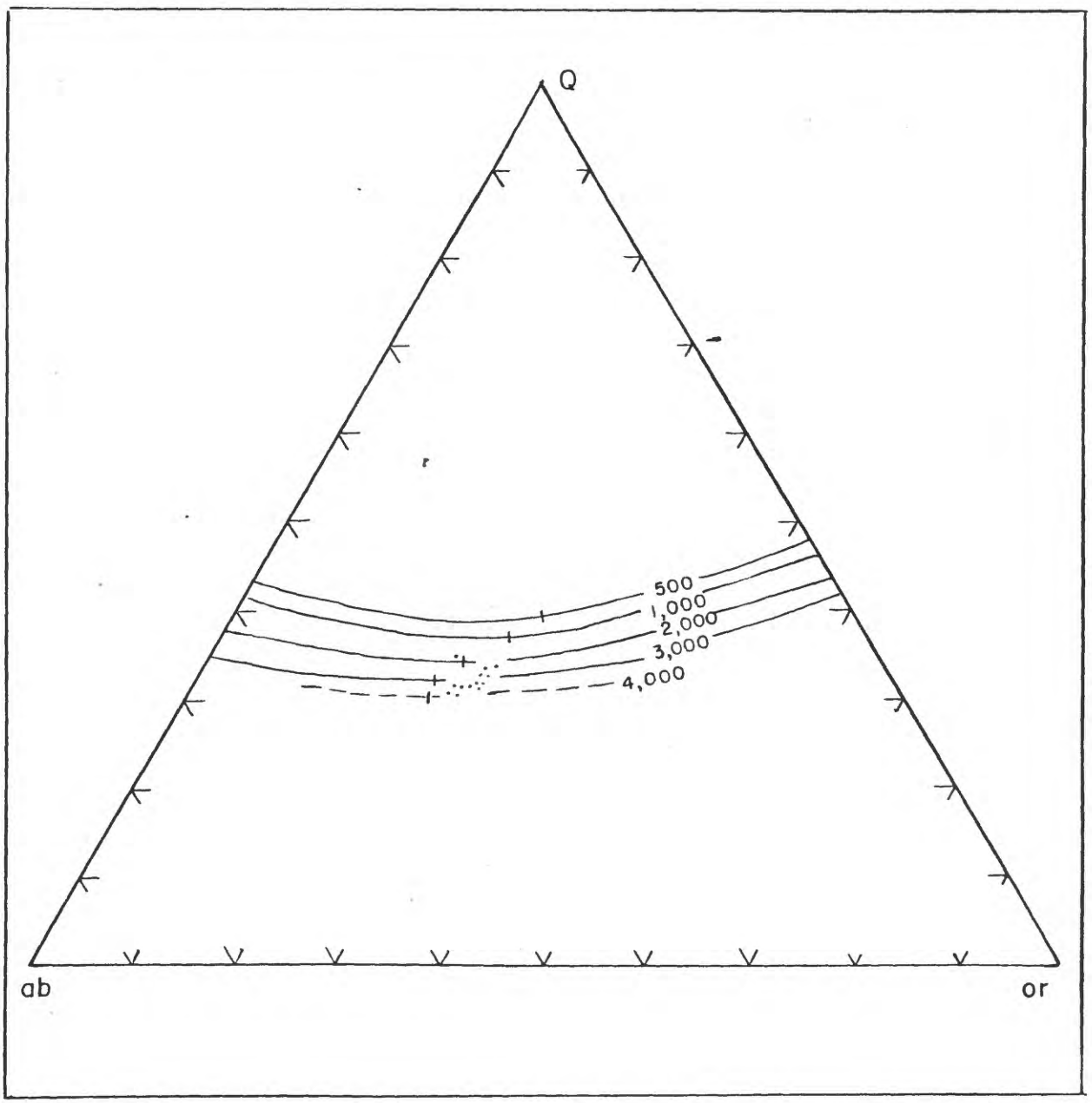

Figure 32.—Equilibrium crystallization diagram for mixtures of albite, orthoclase, and quartz (after Bowen, 1954, p. 10; Tuttle and Bowen, 1958, p. 75). The plots of normative Q, or, and ab from table 6 fall near the minimum-temperature cross bars between the 2,000- and 4,000-atmosphere curves.

the magma is much more complex than the composition of the system on which the diagram is based, and certain components may affect the behavior in unpredictable ways. However, as the system does include most of the major components of the dacite magma, the estimate that the magma formed at a depth of 6½ to 13 kilometers is probably approximately right.

THE PROCESSES OF THE ERUPTION

Eruptive mechanisms

Most students of ash-flow deposits have tentatively concluded that they were erupted and transported by some type of nuée ardente, although most admit that much remains to be learned about the mechanism of eruption and transport. Some authors, however, have proposed other mechanisms of origin, such as froth flows (Kennedy, 1955, p. 495), or certain specialized types of lava flows (Hausen, 1954; Steiner, 1960). Smith (1960, p. 802-810) and Cook (1959, p. 2-6; 1960, p. 135-136) have quite thoroughly discussed the history and development of proposed modes of origin and have explored their various facets and implications, so only a brief outline of the problems will be presented here.

The eye-witness accounts of Anderson and Flett (1903), Lacroix (1904), Perret (1937), and others indicate that a nuée ardente is a turbulent mixture of coarse to fine, incandescent lava fragments and hot gases; it consists of a rapidly moving basal avalanche which contains much gas and most of the solid and liquid material, and it grades upward into a rapidly expanding cloud of gas, ash, and dust. These authors proposed that gas escaping from particles during their flight was either the major cause or an important cause of the rapid transport of material, and held various opinions on the relative importance of gravity and laterally directed explosions as motive forces. Perret (1923, p. 72) stressed the mechanism of continuous escape of gas as a

means of reducing friction between particles, driving them apart, and causing the mass to spread out in the manner of a liquid.

Marshall (1932, 1935) recognized that the constituents of ignimbrites must have reached their site of deposition very soon after their eruption in order to remain hot enough to be welded together, and he proposed that a "nuée ardente of the Katmai type" was capable of transporting the material rapidly enough. Gilbert (1938), Williams (1941, 1954, 1957 and others), Enlows (1955), and many other authors agreed that the most probable mechanism of eruption and transport of deposits containing welded tuff was some type of nuée ardente or glowing avalanche. They recognized, of course, that the eruptions that produced the great ash-flow sheets were many times larger than the observed nuées ardentes of the West Indies and other localities. MacGregor (1952) clarified certain problems and corrected several published misinterpretations of the nuée ardente mechanism. Boyd (1957) has shown thermodynamically that a "tuff flow" is capable of retaining sufficient heat for the particles to become welded when they are deposited.

McTaggart (1960) has proposed a stimulating new hypothesis to explain the mobility of nuées ardentes. First, he concluded from calculations and experiments that the gas escaping from a lava block or particle is not sufficient to support it for more than a small fraction of the time of transport within a nuée ardente. By further experiments he found that the mobility of sand poured down an inclined trough greatly increases with increasing temperature of the sand. He concluded

that the increased mobility is due to rapid expansion of air enveloped and suddenly heated by the sand. He proposed that a similar near-explosive expansion of air temporarily entrapped under and within the hot avalanche of a nuée ardente is a major factor determining its turbulent behavior and its rapid motion. The present writer suspects that gas escaping from lava particles plays a more important role as a lubricant than McTaggart implies, but agrees that suddenly-heated air is probably essential to the nuée's behavior and tremendous speed.

No published accounts have appeared of an observed nuée ardente yielding a deposit containing welded material,[1] so the possibility remains that welded tuff formed by some other mechanism. Hausen (1954) felt that nuée ardente eruptions were not adequate to account for deposits of welded tuff, and proposed that welded tuffs formed from siliceous, gas-charged lavas which were highly mobile due to lubrication by escaping gases. He visualized the internal parts of the flows erupted as a continuous liquid phase. The upper surfaces of such flows were converted to ash by the vesiculating action of escaping gases, and Hausen considers the deposits as only partly pyroclastic. According to his view, welded fluxion structures developed due to flowage along planes of minute vesicles, and these tiny bubbles were stretched, elongated, and collapsed during flowage, but the bulk of material

---

[1]Cook (1959, p. 5) cites a "personal communication" from H. Kuno that the Agatsuma deposit, formed by a nuée ardente at Asama, Japan in 1783, is welded in part. The reference does not state whether this nuée ardente was actually witnessed. H. Williams and G. H. Curtis (oral communication) found partly welded tuff in the lower part of canyons recently cut in the tuff deposit in the Valley of Ten Thousand Smokes. However, no one witnessed the deposition of this tuff.

was never subdivided to form ash (Hausen, 1954, p. 219).

Steiner (1960) has objected to ignimbrites forming from nuées ardentes, and has proposed instead that they formed from lava flows. According to his view, the lava splits into two immiscible liquid phases when it is erupted. One phase, called the "glassy base," is nearly anhydrous and ultimately comprises the shards. The other phase, called the "mesostasis," contains a few percent dissolved water which greatly reduces the viscosity of the lava and permits it to flow freely, somewhat in the manner of plateau basalts. The mesostasis ultimately comprises the dusty material between the shards. The mesostasis separates from the glassy base by vesiculation, and forms vitroclastic textures in a manner similar to vesiculating gas. Steiner uses ingenious reasoning to support certain steps in this process, and if future experimental work supports his conjectures, his hypothesis will merit thoughtful consideration as a possible origin for at least some ash-flow deposits. It is the opinion of this writer, however, that most of Steiner's objections to the nuée ardente hypothesis are based on misunderstandings and misinterpretations, and the writer feels the bulk of field and petrographic evidence favors a nuée ardente type origin for most ash-flow deposits.

History of the ash-flow sheet

The following inferences have been drawn on the mode of origin, eruption, transport, deposition, and cooling of the ash-flow sheet in the Superior-Globe area.

Eruption and transport

The magma, with a chemical composition of quartz latite, may have originated by selective melting at some depth near $6\frac{1}{2}$ to 13 kilometers. As the magma moved upward, it cooled, and crystals of plagioclase, quartz, biotite, sanidine, and other minerals grew. Their proportions indicate a modal composition of dacite. A considerable amount of the partly crystallized magma occupied a chamber in the southwest part of the Haunted Canyon quadrangle at a depth of perhaps 1 or 2 kilometers, and perhaps other chambers lay in the district nearby. As crystallization continued, gas pressure rose, and when about 40 percent of the magma had crystallized, some combination of crustal weakness and mounting gas pressure allowed part of the magma to escape to the surface. Evidence suggests that the eruption issued from a central source, but it is not known whether the orifices were craters, fissures, pipes, or some other form. The initial eruptions were highly charged with gas which escaped with enough violence to thoroughly shatter the magma into ash-size particles, and it is inferred that the material was transported by a nuée ardente type mechanism. Upon eruption, the explosively vesiculating magma rapidly spread laterally in all directions in the form of a gas-charged avalanche. Air was continually engulfed by the incandescent mass, and expanded violently to speed the avalanche forward along its path and to create a constant turbulence within the avalanche. A large billowing cloud undoubtedly rose to great heights, but the bulk of the material was carried by the basal avalanche. Many fragments from the walls of the

vents were carried along with the early eruptions. Successive eruptions rapidly followed the initial outburst.

The successive eruptions were probably individual pulses of activity, perhaps separated by days or even months, but each successive layer was added before the next underlying layer had appreciably cooled. Each individual eruptive pulse added from a few tens to several hundred feet of material to the deposit. The erupted material had sufficient energy and mobility to travel up to 20 miles. The original local relief was moderate, perhaps on the order of 1,000 feet, and the deposits filled in the valleys and ultimately covered the hills under depths of as much as several hundred feet.

As the eruptive series continued, the internal pressure of the gas probably decreased, so that fragmentation of the lava was not as violent as in the initial eruptions, and significant quantities of the lava were of lapilli and block size. Distance of travel, however, did not seem to decrease appreciably. This inference supports McTaggart's (1960) view that mobility of nuées ardentes is mainly due to expansion of entrapped and heated air instead of escaping gases.

When the magma chamber was essentially evacuated, the overlying rock collapsed into it to form a nearly circular caldera about 3½ miles in diameter. The chaotic collapse shattered and deformed the neighboring rocks, and magma locally engulfed large blocks.

Deposition and cooling

The deposited material was a mixture of fragmented lava, intratelluric crystals, and lithic inclusions. The mixture was hot, much of

the lava was still plastic, and the lava fragments continued to slowly emit dissolved gas.

The first-erupted material that came to rest on the pre-volcanic surface was quickly chilled by the ground, and particles became rigid enough to resist deformation. This material formed an insulating blanket so material above it cooled more slowly, and particles retained their plasticity long enough to be deformed and flattened by the weight of the overlying material. The vitrophyre represents a layer in which the particles were plastic enough to become greatly flattened and thoroughly welded together, yet chilled quickly enough to form a glass.

In a thick layer above the vitrophyre the still-plastic particles were deformed by the overlying load and thoroughly welded. Cooling, however, was slower, and the originally glassy constituents devitrified to form the cryptocrystalline, aphanitic groundmass characteristic of the brown zone. The volatiles that continually escaped during the cooling percolated upward, but in the brown zone produced negligible reactions.

The amount of hot gas percolating past a series of successively higher points in the sheet progressively increased, and these streaming volatiles allowed crystallization in the groundmass to proceed beyond simple devitrification. Spherulites, axiolites, and other tiny crystalline forms steadily increased upward in number and size from the brown zone through the gray zone, and into the white zone. Simultaneous with the steadily increasing amount of vapor-phase crystallization was a progressive decrease in the degree of flattening of the lava particles

and blocks because of the decreasing overlying load. As crystallization increased, the outlines of particles became more diffuse. Ultimately, near the top of the sheet in the upper part of the white zone, the particles were essentially undeformed and normolded, and their original outlines were obliterated by crystallization due to long contact with upward-rising hot gases.

The ash-flow deposits that occupied the caldera were subjected to high temperatures and emanating gases for a much longer time than was the bulk of the deposit. A distinctive microcrystalline texture developed in the groundmass of the rocks within the caldera, and some of the rocks were mildly altered by hydrothermal processes.

Post-volcanic history

The region was part of an active tectonic belt, and many faults cut the ash-flow sheet. The faulting may have begun before the sheet had even cooled, and it continued for a long period afterward. The region was uplifted during or soon after the eruptions, for erosion deeply dissected the ash-flow sheet, and active erosion continued long enough to locally remove the entire thickness of the sheet. A period of fluvial deposition followed, during which the Gila conglomerate was laid down in basins and valleys, and the conglomerate rests on eroded surfaces of both the ash-flow sheet and the underlying rocks. Erosion of the ash-flow sheet continued during this fluvial stage, as the Gila conglomerate contains abundant dacitic fragments, and locally both fragments and matrix of the conglomerate were derived entirely from the dacite. Movement along faults continued during and after

the deposition of the Gila conglomerate.

Renewed uplift halted deposition of the Gila, erosion continued to dissect the ash-flow sheet, valleys were cut into the Gila conglomerate, and gradually the present-day topography developed. The combination of extensive faulting and long erosion have produced the present irregular and interrupted distribution of the ash-flow sheet.

CONCLUSIONS

1. The wide areal extent and sheet-like shape of this deposit of silicic composition, the relict and diffuse pyroclastic textures that grade into distinctly pyroclastic textures, the abundant broken phenocrysts, the small angular crystal fragments in the matrix, and the widely distributed pumice blocks and lenticles indicate that the deposit is a pyroclastic rock instead of a lava flow.

2. The deformed and welded shards and lapilli in the lower part of the deposit, the relict outlines of welded textures higher in the deposit, and the progressive downward flattening of pumice fragments indicate that the erupted material retained enough heat to be soft and viscous after coming to rest. This suggests that the deposit is not an air-fall tuff, but instead is an ash-flow deposit that is generally thought to have been transported by some type of nuée ardente.

3. The single trend of zoning, the gradual transitions between zones, the lack of important reversals in flattening ratios of pumice fragments, and the systematic distribution of specific gravity values indicate that the entire deposit was erupted in a short enough time to form a single cooling unit. Slight local contrasts between certain strata suggest that the material was erupted in separate pulses rather than as a continuous, steady outflow, but no single eruption could have cooled appreciably before the next overlying deposit was laid down.

4. The obscuring and obliteration of original textures in the

upper part of the deposit was caused by devitrification and crystallization during the cooling of the mass. It was largely caused by the action of upward streaming volatiles. This action has been considerable because the deposit is much thicker than most single cooling units.

5. The recognition and definition of the three upper zones, and the recognition of the nearly linear relation of the logarithm of the pumice fragment flattening ratio to the stratigraphic level has provided means by which distance below the top of the sheet can be estimated. They also permit the identification of faults within the ash-flow sheet.

6. A likely source for at least part of the ash-flow sheet is a probable caldera defined by a border of intricately faulted and brecciated older rocks and occupied by altered dacite and earlier volcanic rocks.

7. The essentially uniform mineralogy and chemical composition indicate a single magma source. Although only one probable vent has been found, multiple surface sources are not unlikely, but they probably originated from the same magma chamber at depth.

REFERENCES CITED

Anderson, T., and Flett, J. S., 1903, Report of the eruptions of the Soufrière in St. Vincent in 1902 and on a visit to Montagne Pelée in Martinique: Pt. 1, Phil. Trans. Royal Soc. of London, Ser. A, v. 200, p. 353-555.

Bowen, N. L., 1954, Experiment as an aid to the understanding of the natural world: Proc. Acad. Nat. Sciences of Philadelphia, v. 106, p. 1-12.

Bowen, N. L., and Tuttle, O. F., 1950, The system $NaAlSi_3O_8$-$KAlSi_3O_8$-H_2O: Jour. Geol., v. 58, p. 489-511.

Boyd, F. R., 1957, Geology of the Yellowstone rhyolite plateau: Harvard Univ. Ph.D. thesis, 134 p.

Chayes, Felix, 1949, A simple point counter for thin-section analysis: Am. Mineral., v. 34, p. 1-11.

Cook, E. F., 1955, Nomenclature and recognition of ignimbrites (abs.): Bull. Geol. Soc. Amer., v. 66, p. 1544.

_____, 1957, Geology of the Pine Valley Mountains, Utah: Utah Geol. and Mineral Survey, Bull. 58, 111 p.

_____, 1959, Ignimbrite bibliography: Idaho Bur. Mines and Geol., Information Circ. no. 4, 30 p.

_____, 1960, Great Basin ignimbrites: Intermountain Assoc. of Petroleum Geologists, 11th Ann. Field Conf., Guidebook, p. 134-141.

Donnay, Gabrielle, and Donnay, J. D. H., 1952, The symmetry change in the high-temperature alkali-feldspar series: Am. Jour. Science, Bowen volume, p. 115-132.

Enlows, H. E., 1955, Welded tuffs of Chiricahua National Monument, Arizona: Geol. Soc. America Bull., v. 66, p. 1215-1246.

Fenner, C. N., 1923, The origin and mode of emplacement of the great tuff deposit of the Valley of Ten Thousand Smokes: Nat. Geog. Soc., Tech. Paper, Katmai series, no. 1, 74 p.

Gilbert, C. M., 1938, Welded tuff in eastern California: Geol. Soc. America Bull., v. 49, p. 1829-1862.

Goodyear, J., and Duffin, W. J., 1954, The identification and determination of plagioclase feldspars by the X-ray powder method: Mineral. Mag., v. 30, p. 306-326.

Hausen, D. M., 1954, Welded tuffs of Oregon and Idaho: Jour. Mississippi Acad. Science, v. 5, 1951-1953, p. 209-220.

Kennedy, G. C., 1955, Some aspects of the role of water in rock melts: Geol. Soc. America, Special Paper 62, p. 489-504.

Köhler, A., 1941, Die Abhängigkeit der Plagioklasoptik vom vorangegangenen Wärmeverhalten: Min. petr. Mitt., v. 53, p. 24-49.

Lacroix, A., 1904, La montagne Pelée et ses eruptions: Paris, Masson et Cie, 662 p.

MacGregor, A. G., 1952, Eruptive mechanisms—Mt. Pelée, the Soufrière of St. Vincent and the Valley of Ten Thousand Smokes: Bull. Volcanologique, ser. 2, v. 12, p. 49-74.

MacKenzie, W. S., 1957, The crystalline modifications of $NaAlSi_3O_8$: Amer. Jour. Sci., v. 255, p. 481-516.

Mackin, J. H., 1960, Structural significance of Tertiary volcanic rocks in southwestern Utah: Am. Jour. Sci., v. 258, p. 81-131.

Mansfield, G. R., and Ross, C. S., 1935, Welded rhyolite tuffs in southeastern Idaho: Am. Geophys. Union, Trans., v. 56, p. 308-321.

Marshall, P., 1932, Notes on some volcanic rocks of the North Island of New Zealand: New Zealand Jour. Sci. and Tech., v. 13, p. 198-202.

_____, 1935, Acid rocks of the Taupo-Rotorua volcanic district: Royal Soc. New Zealand, Trans. and Proc., v. 64, p. 323-366.

Martin, R. C., 1959, Some field and petrographic features of American and New Zealand ignimbrites: New Zealand Jour. Geol. and Geophys., v. 2, p. 394-411.

McTaggart, K. C., 1960, The mobility of nuées ardentes: Am. Jour. Sci., v. 258, p. 369-382.

Nockolds, S. R., 1954, Average chemical compositions of some igneous rocks: Geol. Soc. America Bull., v. 65, p. 1007-1032.

Orville, P. M., 1958, Feldspar investigations: Carnegie Inst. Washington, Ann. Report of Director of Geophys. Laboratory, 1957-1958, p. 206-209.

Perret, F. A., 1937, The eruption of Mt. Pelée, 1929-1932: Carnegie Inst. Washington Pub. 458, 126 p.

Peterson, D. W., 1959, Origin of the dacite near Superior and Globe, Arizona (abs.): Geol. Soc. America Bull., v. 70, p. 1740.

_____, 1960, Geology of the Haunted Canyon quadrangle, Arizona: U. S. Geol. Survey Quadrangle Map GQ-128.

Peterson, N. P., Gilbert, C. M., and Quick, G. L., 1951, Geology and ore deposits of the Castle Dome area, Gila County, Arizona: U. S. Geol. Survey Bull. 971, 134 p.

Peterson, N. P., 1954, Geology of the Globe quadrangle, Arizona: U. S. Geol. Survey Quadrangle Map GQ-41.

_____, in press (1), Geology and ore deposits, Globe-Miami district, Arizona: U. S. Geol. Survey Prof. Paper 342.

_____, in press (2), Preliminary geologic map of the Pinal Ranch quadrangle, Arizona: U. S. Geol. Survey MF 81.

Ransome, F. L., 1903, Geology of the Globe copper district, Arizona: U. S. Geol. Survey Prof. Paper 12, 168 p.

_____, 1919, The copper deposits of Ray and Miami, Arizona: U. S. Geol. Survey Prof. Paper 115, 192 p.

_____, 1923, Ray Arizona: U. S. Geol. Survey Geol. Atlas, Folio 217.

Rittman, A., 1952, Nomenclature of volcanic rocks: Bull. Volcanologique, Ser. 2, v. 12, p. 75-102.

Ross, C. S., 1955, Provenience of pyroclastic materials: Geol. Soc. America Bull., v. 66, p. 427-434.

Short, M. N., Galbraith, F. W., Harshman, E. N., Kuhn, T. H., and Wilson, E. D., 1943, Geology and ore deposits of the Superior mining area, Arizona: Arizona Bur. Mines Bull. 151, 159 p.

Smith, J. R., and Yoder, H. S., 1956, Variations in X-ray powder diffraction patterns of plagioclase feldspars: Am. Mineral., v. 41, p. 632-647.

Smith, J. V., 1956, The powder patterns and lattice parameters of plagioclase feldspars. I. The soda-rich plagioclases: Mineral. Mag., v. 31, p. 47-68.

Smith, J. V., and Gay, P., 1958, The powder patterns and lattice parameters of plagioclase feldspars. II.: Mineral. Mag., v. 31, p. 744-762.

Smith, R. L., 1960, Ash flows: Geol. Soc. America Bull., v. 71, p. 795-842.

Steiner, A., 1960, Origin of ignimbrites of the North Island, New Zealand—A new petrogenetic concept: New Zealand Geol. Survey Bull. 68, 42 p.

Tuttle, O. F., and Bowen, N. L., 1950, High-temperature albite and contiguous feldspars: Am. Jour. Sci., v. 248, p. 572-583.

_____, 1958, Origin of granite in the light of experimental studies in the system $NaAlSi_3O_8$-$KAlSi_3O_8$-SiO_2-H_2O: Geol. Soc. America Mem. 74, 153 p.

Williams, Howel, 1941, Calderas and their origin: Univ. Calif. Pub., Bull. Dept. of Geol. Sci., v. 25, no. 6, p. 239-346.

_____, 1954, Problems and progress in volcanology: Quar. Jour. Geol. Soc. London, v. 109, p. 311-332.

_____, 1957, Glowing avalanche deposits of the Sudbury Basin: Ontario Dept. Mines Ann. Rept. 1956, v. 65, pt. 3, p. 57-89.

Williams, P. L., 1960, A stained slice method for rapid determination of phenocryst composition of volcanic rocks: Am. Jour. Sci., v. 258, p. 148-152.

Winchell, A. N., 1951, Elements of optical mineralogy, an introduction to microscopic petrography, Part II, descriptions of minerals; Fourth Edition: New York, John Wiley and Sons, 551 p.